3. MORPHOLOGY AND STRUCTURE OF AMAZON CHANNEL[1]

Carlos Pirmez[2] and Roger D. Flood[3]

ABSTRACT

Amazon Channel displays a relatively smooth, concave-up, longitudinal talweg depth profile that suggests a system in equilibrium. The gradual seaward decrease in channel slope occurs despite large variations in the gradient of the valley over which the channel is built. Equilibrium was apparently reached by adjustment of channel slope by two basic processes: changes of channel sinuosity and entrenchment/aggradation of the channel talweg. Channel equilibrium was disrupted in the past, when a knickpoint formed at a channel bifurcation site, associated with the formation of a new channel down-fan and causing a relative base-level drop. The magnitude of base-level drop increases with pre-bifurcation channel sinuosity and with aggradation of the talweg above the adjacent fan. Present-day channel morphology shows that knickpoints would be most pronounced for a bifurcation occurring on the middle fan, and less pronounced on the upper and lower fans. The present longitudinal profile indicates that past knickpoints have largely been erased from the profile. The mechanisms associated with channel equilibrium involved sudden sinuosity changes and channel entrenchment upstream of the bifurcation site, and marked aggradation downstream as a new channel levee formed. Channel bifurcation is related to periods of enhanced channel progradation interpreted to result from increased influx of terrigenous sediment to the fan.

INTRODUCTION

Submarine fans display a network of distributary channels that are the pathways for turbidity currents. The overflow of channelized turbidity currents leads to the formation of levees adjacent to the channel and the accumulation of lens-shaped deposits termed channel-levee systems. Fan growth results from the stacking and overlapping of channel-levee systems, resulting from lateral channel switching, interspersed with mass-flow deposits. It has been suggested from the study of several fans that only one channel-levee system is active at any time during fan growth (Damuth et al., 1983b, 1988; Droz and Bellaiche, 1985; Weimer, 1989). During periods of little sediment input to the fan, such as during the present sea-level highstand, pelagic and hemipelagic sediment blankets the fan surface because terrigenous sediment is prevented from reaching the fan (e.g., Damuth et al., 1988).

Submarine channels on deep-sea fans usually have a sinuous planform. On the mud-rich fans such as the Amazon (Damuth et al., 1983a), Rhône (Droz and Bellaiche, 1985), Mississippi (Garrison et al., 1982; Weimer, 1991), and Indus (Clark et al., 1992), channel sinuosity is commonly greater than 2 with recurving, and some cutoff, meander loops that resemble those of subaerial rivers (Flood and Damuth, 1987; Pirmez, 1994). Flood and Damuth (1987) showed that Amazon Fan channels become more sinuous when traversing steeper valley gradients, resulting in a gradual down-fan decrease of along-channel slope. Flood and Damuth (1987) and Damuth et al. (1988) suggested that channel meandering is largely controlled by the gradient of the valley over which the channels are built, but that other factors such as the frequency and type of sediment load of turbidity currents may also constitute important controls on channel meandering. This suggests that the channels seek a graded, or equilibrium, profile in which slope is adjusted so that the turbidity currents are in equilibrium with the sediment load. Because each fan channel is generally perched atop its own channel-overbank deposits (Damuth et al., 1988) and the channel floor elevated in respect to the surrounding fan surface, a bifurcation may result in the disruption of the equilibrium profile with the introduction of a knickpoint at the site of channel switching. Knickpoints on the channel depth profile will result in slope changes along the turbidity current pathways that may directly affect the flow and consequently the manner in which sediments are distributed on the fan (Flood et al., 1991). A detailed analysis of the morphology and internal structure of the channel may provide clues as to the effects of past bifurcations and possibly on the mechanisms through which the channel morphology adjusts to varying conditions.

Amazon Channel is the youngest channel-levee system within the distributary channel network of Amazon Fan (channel 1 of Damuth et al., 1983a; Fig. 1). The channel was surveyed in detail, with almost 100% SeaBeam coverage, closely spaced seismic reflection profiles (water-gun and 3.5 kHz), and several piston cores (Manley and Flood, 1988; Flood et al., 1991; Pirmez, 1994). It is a continuous channel system that is directly connected to Amazon Canyon on the outer shelf and that extends for at least 900 km into abyssal depths. The path of Amazon Channel developed as a result of numerous channel bifurcations (Fig. 1). In each of these events, turbidity currents flowed to the low-lying valleys adjacent to the channel-levee system, and a portion of the channel became abandoned as a new channel-levee system developed downstream. The upstream segment of the channel remained active after a bifurcation, and was continuously reused as a pathway for the turbidity currents redirected to the new channel system downstream. As a result, different segments of the channel reflect a different growth history, and the upstream portions of the channel underwent a longer period of development compared to the lower segments. Bifurcations were interpreted to occur by avulsion (Damuth et al., 1983b, 1988; Manley and Flood, 1988), that is, by sudden abandonment of a portion of the channel as a result of levee breaching.

In this paper we present the results of measurements of Amazon Channel morphology combined with the interpretation of seismic reflection profiles. We first describe briefly the main morphologic parameters of the channel and how they relate to each other. The main

[1]Flood, R.D., Piper, D.J.W., Klaus, A., et al., 1995. *Proc. ODP, Init. Repts.*, 155: College Station, TX (Ocean Drilling Program).
[2]Lamont-Doherty Earth Observatory, Columbia University, Palisades, NY 10964, U.S.A.
[3]Marine Sciences Research Center, State University of New York, Stony Brook, NY 11794-5000, U.S.A.

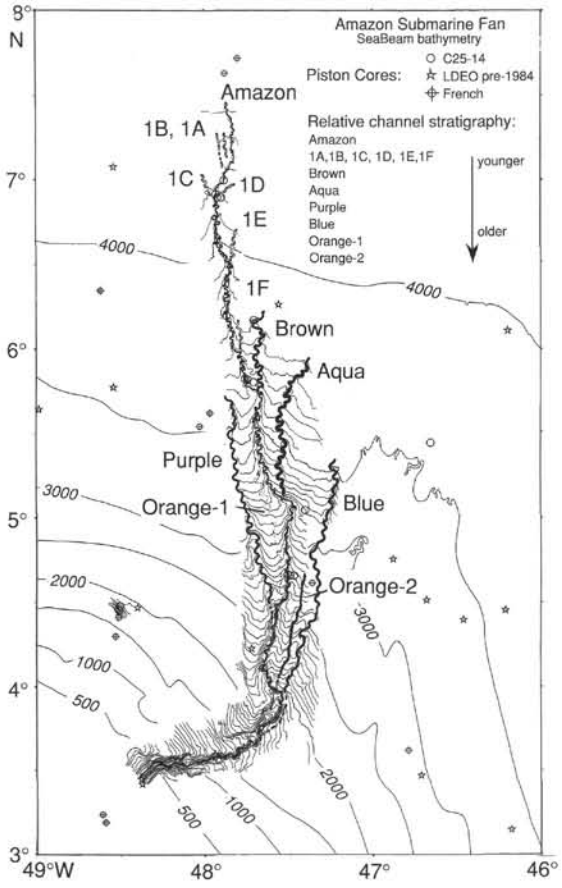

Figure 1. Amazon Fan bathymetry including SeaBeam coverage of Amazon Channel. Channel stratigraphy according to the nomenclature of Manley and Flood (1988) and Pirmez (1994). Bathymetry in uncorrected meters (v = 1.5 km/s). Map modified from Flood et al. (1991).

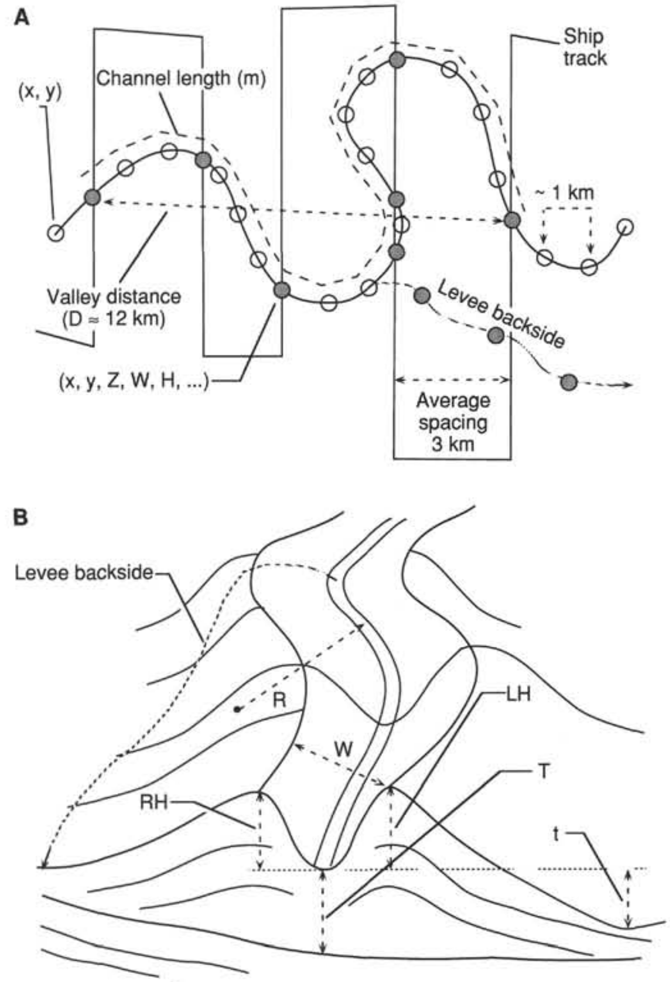

Figure 2. Scheme of channel measurement procedures. **A.** Channel length was determined by adding the distance between every point digitized (open and filled circles). Channel parameters (talweg depth = Z, width = W, relief = H, etc.) were measured at ship track crossings (filled circles). Valley slope is equal to $\Delta Z/D$ and channel slope is equal to $\Delta Z/M$. **B.** Channel relief (H) and width (W) are measured along a line perpendicular to the overall channel path at the highest point outside the channel (levee crest). Channel relief is average of left (LH) and right (RH) values. Basal levee unconformity (defined by onlap of channel-levee reflections, thick line at bottom), serves as the reference for total aggradation (T). Topographic aggradation (t) is measured where a line perpendicular to the overall channel path reaches the lowest point outside the channel (interchannel low). The levee backside profile is determined by the path of steepest descent outside the channel (also projected in A). Depths and thickness are converted from two-way time using a constant sound velocity (1.5 km/s).

goal of investigating the spatial variation and cross-correlation of different morphologic parameters is to gain insight into the processes that shape channel morphology. We then interpret seismic reflection data to reconstruct the channel geometry surrounding bifurcation sites and to map the spatial and temporal distribution of sedimentary sequences. The geometry and acoustic character of the seismic sequences may provide insights into the causes and effects of channel bifurcation on the channel morphology and depositional sequences.

DATA AND METHODS

Amazon Channel morphologic parameters were measured using digital SeaBeam bathymetric profiles (center beam) and large scale (40 in./degree, ~1:109,368 at the Equator) bathymetric maps produced from SeaBeam data. The length of the channel was calculated by adding the straight line distances between digitized points (~0.1 km apart on average) in the center of the channel. Channel measurements performed on individual bathymetric and seismic profiles were linked to the coordinates of the corresponding (or closest) ship track crossing of the channel (Fig. 2A). The measurements could then be displayed in respect to distance along the sinuous channel.

Channel parameters measured and calculated are (Fig. 2A, -B): talweg depth (Z, negative down), channel width (W) and relief (H), talweg topographic (t) and total (T) aggradation, channel (S_c) and valley (S_v) slope, sinuosity (P), and channel form ratio (F). W and H are measured between levee crests and represent bankfull values, channel width represents the average of the left (LH) and right (RH) sides of the channel (Fig. 2B). F is the width:relief ratio of the channel cross section (F = W/H). Valley slope is calculated between two Z measurements separated by a straight "ruler" with length D ≈ 12 km ($S_v = \Delta Z/D$; Fig. 2A). Channel slope is calculated between the same Z values but using the along-channel distance M ($S_c = \Delta Z/M$). Channel sinuosity is simply the slope ratio S_v:S_c, which is equivalent to the distance ratio M:D. P, S_v, and S_c are assigned to the midpoint of the channel segment measured. The ruler is advanced along the channel by a fixed distance (4 km along channel) and the calculation repeated in a sliding scheme. The chosen ruler length corresponds to 2 to 3 times the average meander wavelength (Pirmez, 1994). Increasing D beyond 12 km results in stronger smoothing of the channel parameter variations along channel. Conversely, sliding distances smaller than 4 km and small ruler lengths tend to enhance small errors in the digitized channel shape and depth measurements. Topographic aggradation represents the net elevation of the talweg (or levee crest) in respect to the adjacent fan surface, measured along a line perpendicular to the valley orientation (Fig. 2B). Total aggradation corresponds to the thickness of deposits beneath the talweg to the base of the channel-levee system (basal unconformity on seismic profiles). The path a parcel of flow would follow once leaving the channel is characterized by first drawing the path perpendicular to the levee-backside bathymetric contours and then measuring its length and depth (Fig. 2A, -B). The levee backside profiles begin at a point on the channel talweg, but have distance-depth values that are independent of the channel talweg profile. Details of methodology, evaluation of potential errors and other measurements such as meander shape, wavelength, amplitude, radius of curvature, and cross-channel relief difference are discussed elsewhere (Pirmez, 1994).

Seismic reflection data were acquired with a dual water-gun source (2×80 in.^{3}) and a four-channel streamer. Seismic data were processed with band-pass filtering (30–180 Hz), automatic gain control (100 ms window, 10% gain applied), trace amplitude equalization (100 trace window), and displayed with variable area (positive peaks only). This processing highlights lateral continuity of reflections at the expense of preservation of true amplitudes, although relative changes in amplitude are still preserved.

CHANNEL MORPHOLOGY

At several locations Amazon Channel abruptly changes orientation (Figs. 1, 3A–3D), corresponding to the sites where a bifurcation occurred. The abandoned channel segments from which Amazon Channel bifurcated were given color names by Manley and Flood (1988) and are identified in Figures 1 and 3. Several small channels have been identified on the lower portion of the channel and are named 1F to 1A in order of decreasing age (Figs. 1, 3D; Pirmez, 1994). The youngest channel path is called Amazon Channel. The bifurcation sites and paths of the abandoned channels are deduced from the channel morphology and interpretation of the seismic reflection data (Manley and Flood, 1988; Pirmez, 1994; and below).

Longitudinal Depth Profile

The longitudinal depth profile is a relatively smooth, concave-up function of distance along the channel, suggesting a system in equilibrium. The measured channel extends for 807 km between the first and last SeaBeam survey crossings. Distances along the channel are referenced to the first survey crossing (0 km mark; Z = –928 m). The system extends an additional 60 km from the 0 km mark to the –100 m bathymetric contour (Figs. 3A, 4). The canyon crosses the shelf break at the –12 km mark (Z = –700 m, Fig. 4), and its surface expression on the shelf extends up to the –75 m bathymetric contour, landward of which it becomes buried by the pro-deltaic sediments of the Amazon subaqueous delta (Nittrouer et al., 1986). On the lower fan, small unleveed channels of low relief (< 10 m) are observed beyond the SeaBeam survey (Damuth et al., 1983a; Moyes et al., 1978), but these channels cannot be confidently connected to Amazon Channel.

Aggradation

The talweg cuts below the adjacent shelf and slope until the 60 km mark, defining the seaward limit of Amazon Canyon (Figs. 3A, 4, 5). Between 60 and 100 km levees develop above the adjacent fan surface, marking the canyon-channel transition region (Fig. 5). Amazon Channel can be subdivided by its topographic aggradation characteristics: an upper fan channel with levees above the adjacent fan but with a talweg at the same level or below the fan surface; the middle fan channel where both talweg and levees are perched above the adjacent fan; and the lower fan channel with the same aggradation characteristics as on the upper fan (Fig. 5).

Channel Width and Relief

Maximum relief is observed within the canyon, immediately down slope of the shelf break (Fig. 6A). Relief decreases to a minimum of about 150 m at the beginning of the canyon-channel transition zone (~60 km), and increases to a maximum of about 200 m at the end of the transition region (~100 km; Fig. 6A). Relief decreases down to about 40 m at the 700 km mark, beyond which there is pronounced decrease to a minimum of about 7.5 m at the end of the surveyed channel. Superimposed on the overall decrease in channel relief, there are regions where the channel becomes markedly shallower. For example, between 220 and 340 km, relief decreases rapidly, reaching a local minimum of about 35 m, and increases again to about 85 m at the 390-km mark (Fig. 6A). Local minima in the relief distribution are also noted near the 450-, 530-, and 640-km marks. Marked decreases of channel relief may result from talweg infilling or erosion of the levee crests. Conversely, a down-fan relief increase may result from talweg entrenchment (degradation) or growth of the levees at the expense of the talweg.

The transition from canyon to channel is marked by a pronounced decrease in width (Fig. 6B), and this may have been an important control on the spatial development of turbidity currents (Pirmez, 1994). Channel width decreases within the upper portion of the channel to about 1.5 km near the 370-km mark, and varies little, between 0.8 and 1.3 km, over the middle portion of the channel (Fig. 6B). The lowermost portion of the channel shows an overall increase of channel width, reaching up to 1.8 km near the end of the surveyed channel.

Slope and Sinuosity

Channel slope decreases from 8 m/km to 1 m/km at the end of the surveyed channel (Fig. 7A). The profile is rather irregular within the canyon, reaching a maximum slope of 15 m/km near the shelf break and rapidly decreasing to 8 m/km at the canyon-channel transition, where there is no change in slope. Even though the longitudinal depth profile (Fig. 4) is relatively smooth, close examination of the channel slopes indicates the presence of several knickpoints (Fig. 7A). Across the knickpoints, channel slope increases in the downstream direction by up to 50%. Knickpoints on the upper half of the channel generally show relatively minor slope increases of 15% or less, with the exception of that observed near the 170-km mark, where slope increases by 40% across the knickpoint (Fig. 7A). In contrast, the lower half of the channel has about six knickpoints where the proportional increase in slope across the knickpoints is greater than 20%, including the most pronounced knick at 700 km. The valley slope is much more variable, with large changes occurring in particular near the bifurcation sites (Fig. 7A). The valley slope reflects to a large extent the fan surface over which the channel developed, but also reflects changes in talweg elevation due to aggradation, infill, and entrenchment. In this sense, valley slope in the submarine fan is analogous to valley slope in the fluvial environment. Valley slope shows pronounced maxima that tend to occur upslope of the bifurcation points. At the bifurcation sites, valley slope is either a minimum (e.g., Blue, Brown; Fig. 7A) or is rapidly decreasing (e.g., Aqua, 1E; Fig. 7A).

Amazon Channel sinuosity is smaller than 1.5 over most of the upper half of the channel (Fig. 7B). From 350 to 400 km, sinuosity increases to about 2.3, and varies between 1.2 and 2.7 for the remainder of the channel. Nine meander cutoff loops are identified between 390 and 670 km where sinuosity is greatest (location in Fig. 7B). A

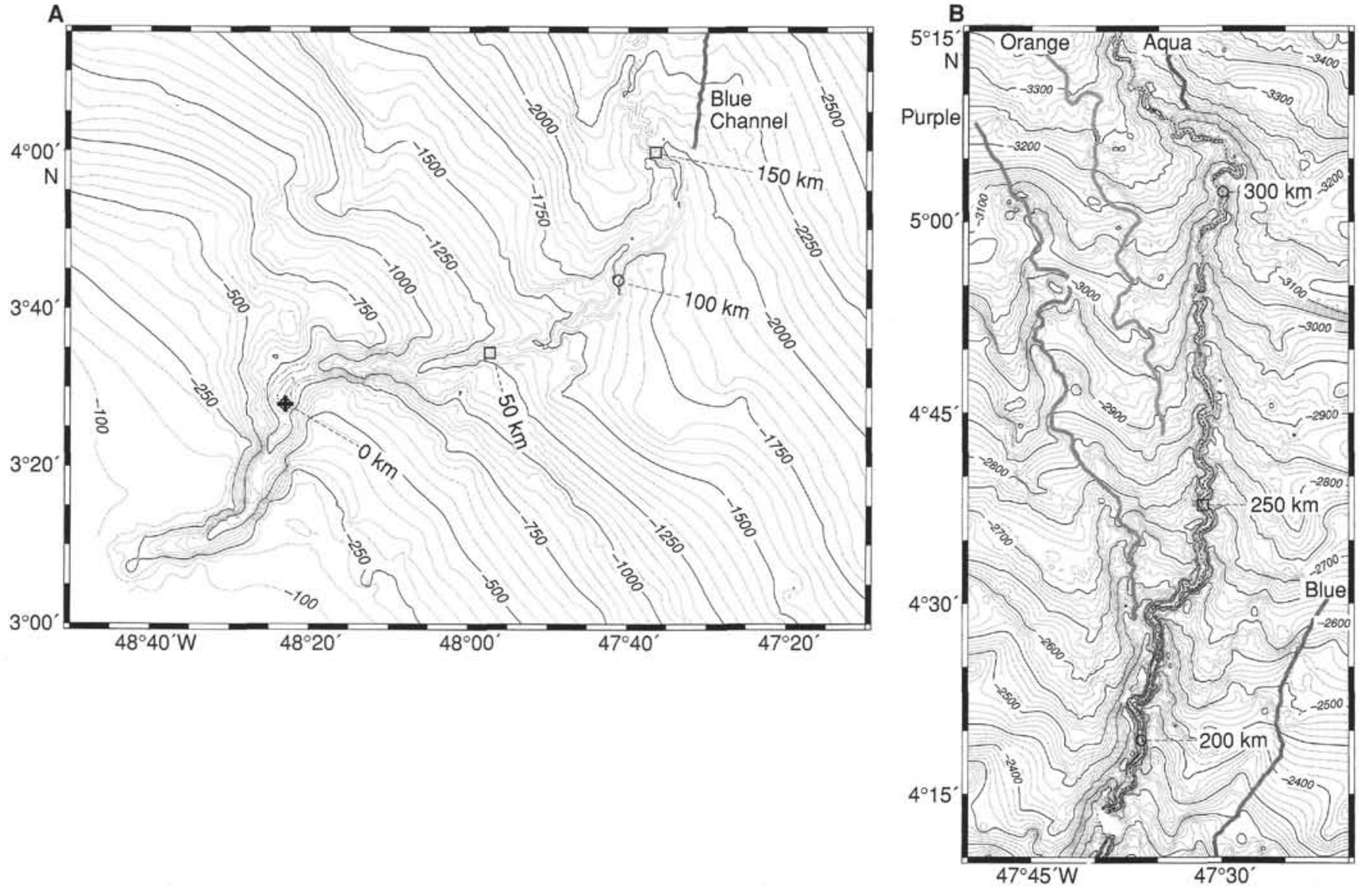

Figure 3. Bathymetry of Amazon Channel gridded and contoured (Wessel and Smith, 1991) from digital SeaBeam data. Distance marks are placed every 50 km (alternating circles and squares) for easy reference with graphs presented in subsequent figures. The "zero" mark was set to the first ship track crossing of the channel during cruise RC-2514 (cross). The digitized path of Amazon Channel is indicated by a thin dashed line, and the paths of the abandoned channels (partly or completely buried, based on bathymetric and seismic data) are indicated by gray lines with the respective names. Grid interval was specified in fractions of a nautical mile (1 nmi = 1852 m) and parameters for each grid are: **(A)** canyon and upper fan, grid interval (GI) 0.5 nmi, contour interval (CI) of 50 m; **(B)** and **(C)** upper and middle fan, GI of 0.15 nmi, CI of 10 m; **(D)** middle and lower fan, CI of 10 m, map was manually contoured based on SeaBeam derived data.

few other meander cutoff loops can only be tentatively identified because they are either buried or within older channel segments (see below). Channel sinuosity shows a good correlation with valley slope, although there is significant scatter (Fig. 8; also Fig. 7A, -B). For $S_v > 8$ m/km, sinuosity is low, mostly less than 1.5. For 3 m/km $< S_v <$ 7 m/km, sinuosity tends to increase markedly, with a maximum sinuosity at $S_v \approx 4$ m/km. For $S_v < 3$ m/km, sinuosity is mostly smaller than 1.8 m/km. Scatter about these trends appears to be in part related to recent channel adjustment, such as in the region across a meander cutoff at the 390-km mark (Figs. 3C and 8). The P–S_v relation for Amazon Channel suggests that there exists a particular range of gradients that favors submarine meander development, or a "meandering field," to use the analogy with fluvial systems (Schumm, 1977).

The channel system developed over a fan surface with large variations in valley gradient. Despite these variations, the longitudinal channel profile displays proportionately small changes in gradient. The difference between valley and channel slope requires that there are mechanisms by which the channel maintains a relatively smooth decrease in channel slope down-fan. The variations in sinuosity along the channel suggest that channel gradients are largely adjusted by planform changes, as suggested previously by Flood and Damuth (1987). In this manner, a more sinuous planform is the apparent response of the channel to a steep valley gradient, as if the channel attempts to maintain a constant or gradually decreasing slope.

Along most of the channel, a local increase in valley gradient from one channel segment to the next downstream corresponds to an increase in channel sinuosity and vice-versa (Fig. 8). Overall, the correlation lines rotate toward the vertical, as channel gradient decreases in the down channel direction (dashed lines in Fig. 8). In this manner, we may interpret the P–S_v distribution as indicating that the equilibrium slope decreases in the downstream direction (Flood and Damuth, 1987). Where slope and sinuosity are positively correlated, the channel is interpreted to be in equilibrium in the sense that adjustments to spatial variations in valley slope occur via changes in the planform sinuosity (i.e., without aggradation or degradation). Segments where there are rapid spatial variations in channel slope display negative correlation between P and S_v and are interpreted to be out of equilibrium (dark stripes in Fig. 7). About 80% of the channel length displays a positive P–S_v correlation from one segment to the next. The negatively correlated segments occur predominantly on the lower half of the channel as well as in the canyon. This is also the relatively younger portion of the channel, which may still reflect talweg irregularities associated with recent bifurcations and meander cutoff loops or with structural control in the canyon.

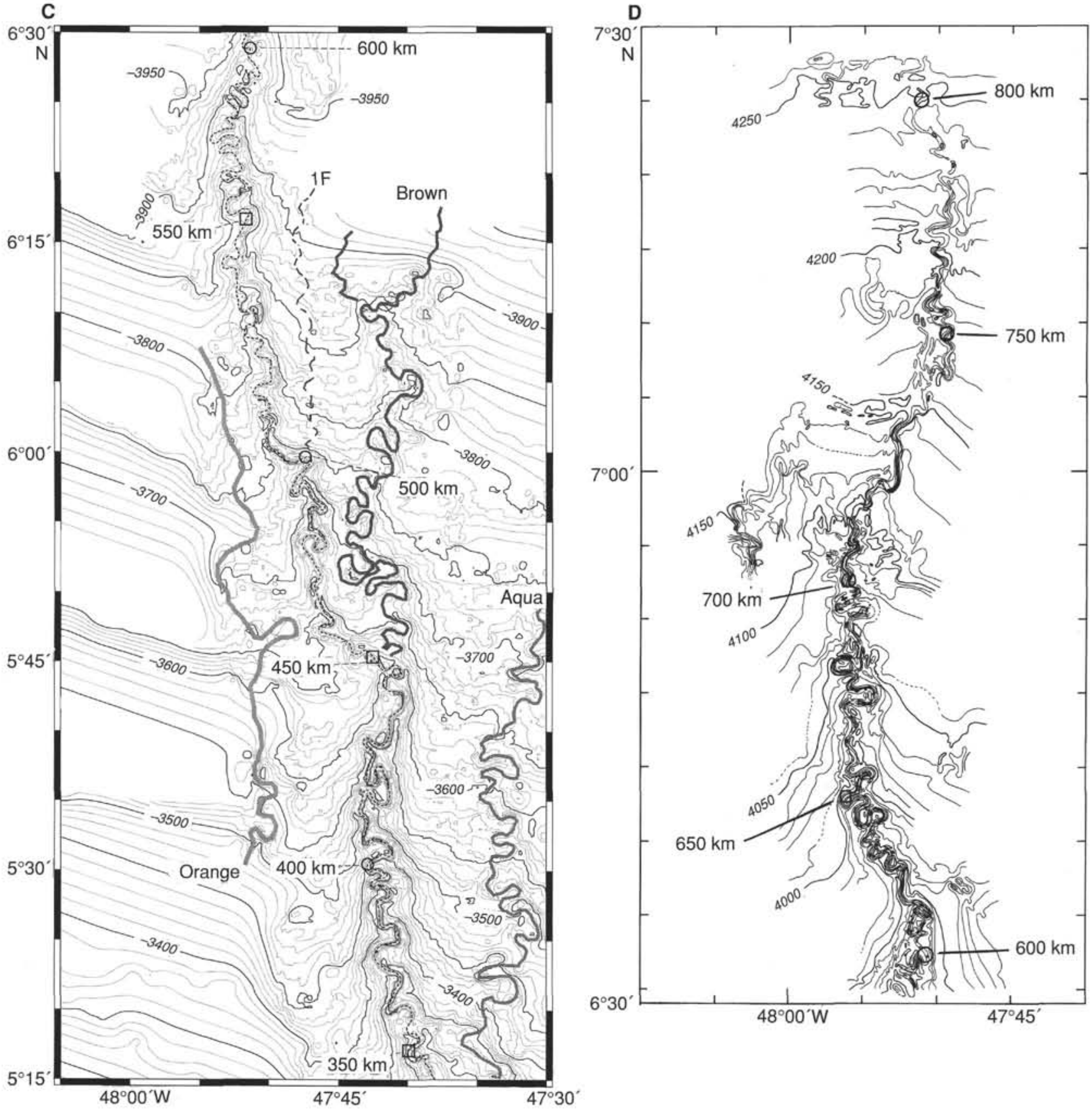

Figure 3 (continued).

Channel Form Ratio

The width:relief ratio (F) of Amazon Channel varies between 10 and 40 for most of the channel, except beyond 700 km where a pronounced trend of channel shallowing and widening leads to large F values at the end of the surveyed channel (Fig. 9A). Between about 300 and 700 km, F ratios reflect primarily changes in channel relief, because width varies relatively little (Fig. 6A, -B). F ratios show a remarkable anti-correlation with channel sinuosity (Fig. 9A, -B). This is the same type of relationship observed in river channels (Schumm, 1977).

Because on the middle fan channel F values reflect primarily variations in channel relief, the changes in form ratio may indicate vertical variations of the talweg position associated with entrenchment/aggradation of the channel. For instance, the smallest form ratios along Amazon Channel are observed near the 390-km mark (F ~ 10; Fig. 9A). This is also the region where a meander cutoff loop is observed. This is the only oxbow loop (Fig. 3C) with a floor above the present talweg of Amazon Channel, suggesting that the channel may have entrenched after meander cutoff (Pirmez, 1994). This suggests that the equilibrium profile of the channel is maintained by both changes in planform sinuosity and by the redistribution of channel sediments through talweg entrenchment and aggradation.

Levee Backsides and Longitudinal Profile

The perched nature of the channel talweg suggests that it is located in a naturally unstable position because the deeper interchannel

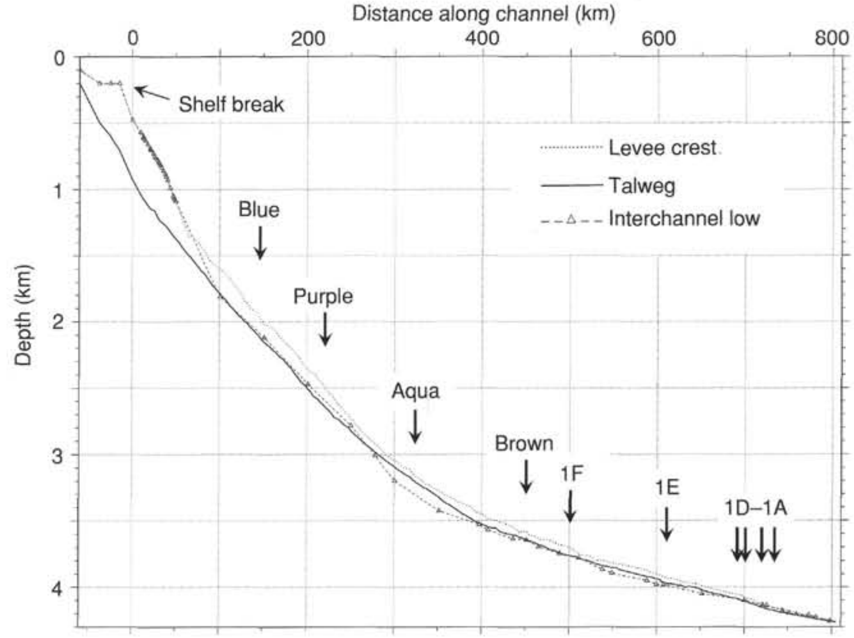

Figure 4. Longitudinal depth profile of Amazon Channel. Arrows point to the along-channel location of channel bifurcations. Talweg depth profile is overall smooth and concave to the sea surface suggesting a graded system, although knickpoints are noted in the vicinity of bifurcation sites and meander cutoff loops (see below). Note the onset of levee development at 60 km, where the talweg and levee crest approach the adjacent fan surface (interchannel low).

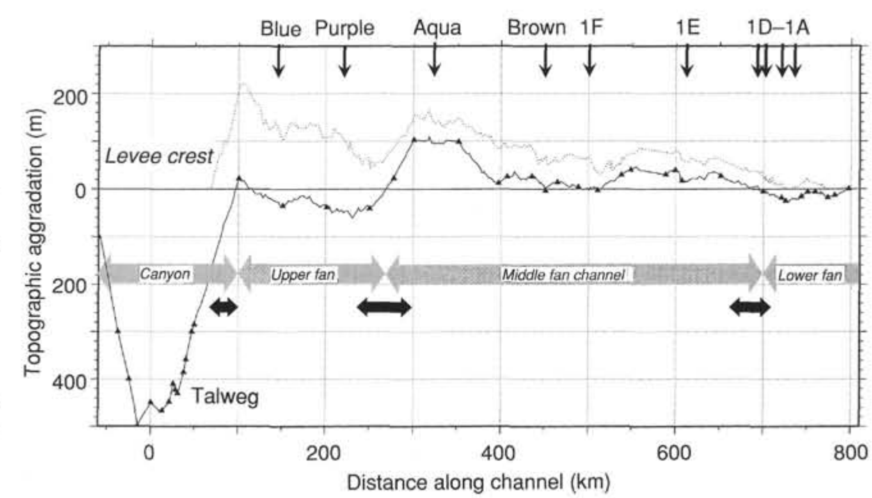

Figure 5. Channel topographic aggradation is the difference between the depth of the talweg (line with triangles) or the levee crest (dotted line) and the depth to the adjacent interchannel topographic low. The buildup of levees above the adjacent fan between 60 and 100 km marks the canyon-channel transition region. On the upper fan the levees are above the adjacent fan surface, but the talweg sits at or below the adjacent fan surface, whereas on the middle fan the talweg is at the same level or perched above the adjacent fan. The talweg cuts down below the adjacent fan surface beyond about 700 km, where only small levees build above the adjacent fan.

depression constitutes a more favorable route to dissipate the energy of channelized flow. This is illustrated by plotting the longitudinal talweg depth profile together with the levee backside topography (Fig. 10). The backside profiles indicate the potential effects of a bifurcation on the longitudinal depth profile of the channel. The profiles indicate that for a breached channel to become completely abandoned, the breach in the levee has to be at least as deep as the whole channel relief; otherwise the longitudinal profile of the parent channel still remains the easier route (arrows in Fig. 11A, -B). Based on the levee backside profiles, the avulsion process in the submarine channels implies insignificant amounts of erosion across the levees. This is particularly evident on the upper portion of Amazon Channel where the levees are often wide (Fig. 11A). Flow stripping will be facilitated if there is a breach or gap on the levees (Fig. 11B), but for the channel to avulse, the gap must be deeper than the talweg. Alternatively, the channel talweg becomes filled, in which case a flow will directly follow the backside route.

Backside gradients average 20 to 50 m/km (1°–3°), but near the levee crest, gradients reach 80–120 m/km (5°–7°). The profiles follow a concave-up curve, with gradually decreasing gradients until approaching the interchannel topographic depression (Figs. 10, 11). These gradients are much larger than the slope along the channel talweg and show that if a bifurcation occurred on the present-day channel, a significant knickpoint would be introduced on the longitudinal depth profile. For example, the profiles near the 500-km mark along the channel (Fig. 11B) show that the backside path falls off by about 150 m in only 20 km, with an average slope of 7.5 m/km, whereas the average Amazon talweg gradient is only about 2 m/km (Fig. 7A). Average backside slopes are three to four times greater than the average channel gradient near the profile. Knickpoints with such a large increase in gradient are not observed on the present-day longitudinal profile. Thus, if we assume that the present-day morphology is representative of past conditions, knickpoints associated with past avulsions must have been largely erased from the longitudinal profile.

The backside profiles on the upper portion of Amazon Channel (e.g., between 150 and 250 km; Figs. 10, 11A) are also much steeper than the channel gradient, in particular in the portion of the levee edifice above the talweg. However, because the talweg is on average close to or slightly below the adjacent interchannel depression, the backside path provides little topographic advantage in comparison

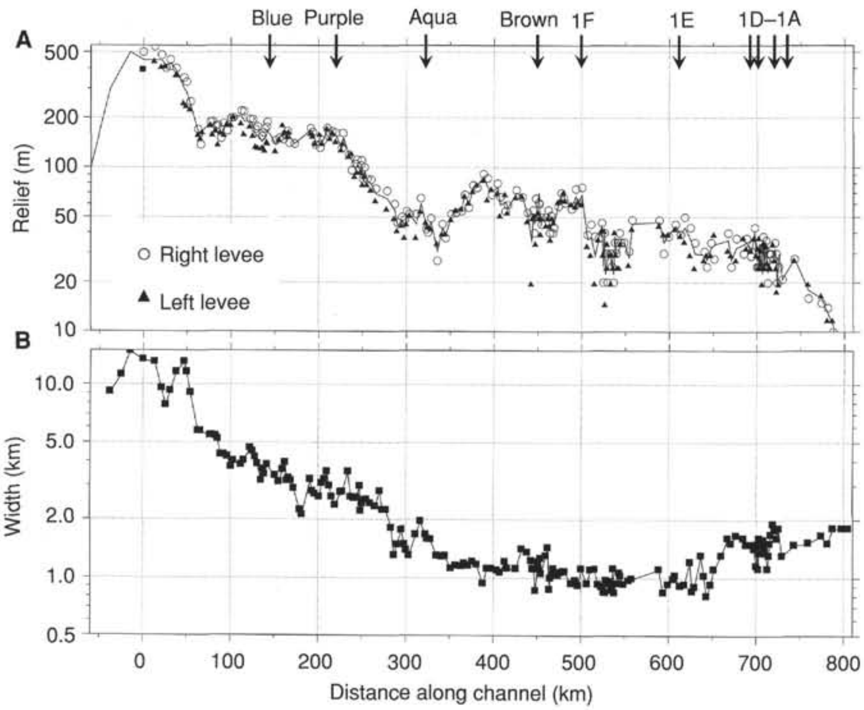

Figure 6. Amazon Channel dimensions. **A.** Mean channel relief (line) decreases down-fan from a maximum of 500 m near the shelf break to less than 10 m at the end of the survey. Along channel variations in channel relief reflect changes in the balance between levee growth and talweg aggradation. Talweg entrenchment appears to occur where relief increases down-fan (e.g., between 340 and 400 km, cutoff meander discussed in text occurs at 390 km), talweg aggradation appears to dominate where relief decreases faster down-fan (e.g., between 220 and 300 km). **B.** Width decreases by a factor of 2 within the canyon, and an additional decrease from 5 to 1.5 km is noted on the upper fan. Middle fan channel width remains approximately constant and increases in the lower fan.

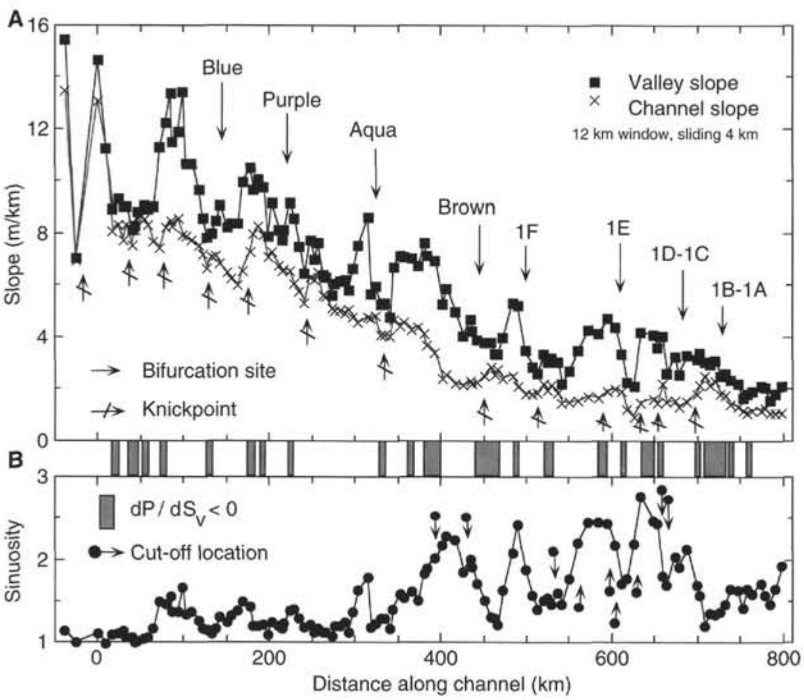

Figure 7. Computed morphologic parameters of Amazon Channel. **A.** Channel slope shows an overall decrease along the channel punctuated by relatively rapid down-fan increases, or knickpoints. Valley slope increases markedly upstream of bifurcation sites and decreases rapidly across the site. The occurrence of peak valley slope upstream of a bifurcation site is interpreted to reflect headward erosion subsequent to a bifurcation. **B.** Channel sinuosity (ratio of valley to channel slope) reflects the underlying changes in valley slope with maximum sinuosity occurring upstream of bifurcation sites. Location of meander cutoff loops is approximately coincident with the knickpoints observed on the talweg profile. Dark bars between the two graphs indicate segments where channel slope changes rapidly and the channel appears out of grade (see text for discussion). These segments tend to be longer and more frequent toward the younger, lower portion of the channel.

with the present-day channel talweg. Practically no knickpoint would be introduced on the longitudinal profile near the breached point, although an increase in slope may develop farther down-fan due to regional topographic variations alongside the channel. If the present-day conditions on Amazon Channel are representative, for an avulsion to occur on the upper fan either a catastrophic event must remove the levee or the channel must be filled prior to bifurcation. On the lower portion of the channel, where aggradation is relatively small (Figs. 4, 5A), the interchannel depression offers little topographic advantage over the talweg. Where the channel cuts below the adjacent fan surface beyond 700 km, an avulsion will require that the channel be filled first, so that the talweg is raised to at least the same level of the adjacent fan. Because of the large topographic aggradation and high channel sinuosity, the largest increase in gradient would result from a bifurcation in the middle fan (Figs. 10, 11B).

CHANNEL BIFURCATIONS

The morphology of Amazon Channel suggests the types of mechanisms involved in maintaining an equilibrium profile, namely changes in planform sinuosity and talweg elevation through en-

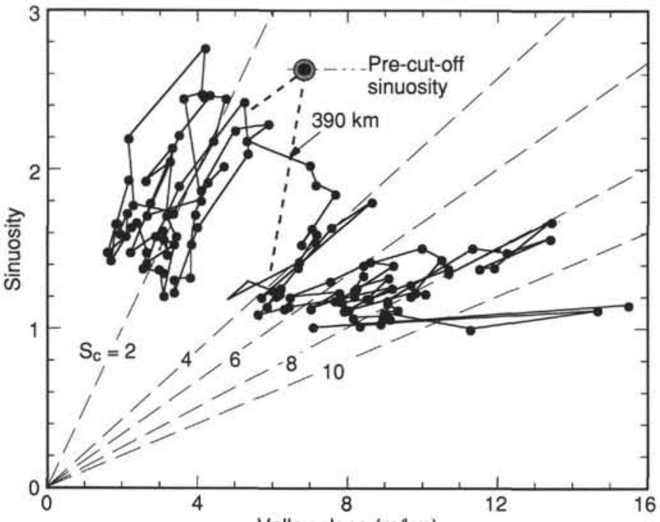

Figure 8. Cross-plot between valley slope and sinuosity. Points represent individual measurements spaced about 12 km apart, connected by lines following the channel down-fan. An overall counter-clockwise rotation of the correlation lines reflects a gradual down-fan decrease in the equilibrium channel slope (S_c, in m/km, dashed lines). Most of the channel shows a positive correlation between sinuosity and valley slope, suggesting that sinuosity change down-fan (and possibly through time as well) is an important mechanism to maintain graded conditions. Segments where channel slope changes rapidly display a negative correlation between valley slope and sinuosity (marked by dark bands in Fig. 7), indicating that entrenchment/aggradation must be playing a role in adjusting the longitudinal profile. The most prominent of these segments occurs across a hanging cutoff meander near 390 km along the channel. The larger circle and lines indicate the situation prior to the meander loop cutoff.

trenchment and aggradation. It also suggests that, given the relatively small slope increase across knickpoints observed on the longitudinal depth profile, equilibrium was largely reattained after disruption by past bifurcations. Investigation of the morphology and structure near past bifurcations is needed to determine the history of channel development before and after channel bifurcation, and the extent to which past bifurcations disrupted channel equilibrium. We will first examine a recent channel bifurcation on the lower fan, and then analyze the morphology and structure of older bifurcations on the upper and middle fan.

Lower Fan Bifurcation

Amazon Channel bifurcated from the 1C channel near the 700-km mark (Fig. 12A). Near the site of bifurcation we note a wide levee to the west of Amazon Channel that suggests the presence of a buried, possibly cutoff meander in the vicinity of the bifurcation site (Fig. 12B). Channel sinuosity is high upslope of the bifurcation site and decreases rapidly across and downslope of the 700-km mark (Figs. 12A, 7B). The acoustic echo character also shows an abrupt change near the bifurcation, from higher acoustic penetration and acoustically layered levees upstream (Fig. 13A) to acoustically prolonged levee reflections downstream (Fig. 13B, -C). This suggests an increase in the content of sand in the near surface sediments, supported by piston core data (Flood et al., 1991; Pirmez, 1994). The 3.5-kHz profiles indicate that the 1C channel is now partially filled (Fig. 13B), although the timing of the fill with respect to the bifurcation cannot be resolved. The Amazon Channel talweg (1B phase) cuts into a surface (marked "B" in Fig. 13B) that corresponds to the top of the abandoned 1C levee.

Amazon Channel morphologic parameters across the bifurcation site show that a pronounced knickpoint occurs just upslope of the site of bifurcation (Fig. 14A; 698 km, 6°52.5′N in Fig. 12B). Channel slope increases significantly across the knickpoint, but the small increase of averaged valley slope from 680 to 700 km may be due to the talweg being at about the same level as the adjacent fan prior to bifurcation (Fig. 14B). The knickpoint may also be in part related to a sudden decrease of sinuosity as suggested by the apparently cut off meander near the site of bifurcation (Figs. 14C, 12B). Channel width and relief (Fig. 14D, -E) are variable but consistently indicate relatively small F ratios (Fig. 14F), corroborating the interpretation of channel entrenchment across the bifurcation site (Fig. 13B).

The observations near this lower fan bifurcation indicate that the channel is in a state that still reflects the disruption of its original equilibrium profile. The knickpoint did not migrate significantly upslope from the bifurcation site, but relatively coarse-grained sediments were deposited downstream from the bifurcation site (Fig. 12A; Flood et al., 1991). The relatively steep channel slope observed downstream of the bifurcation site could be related to rapid deposi-

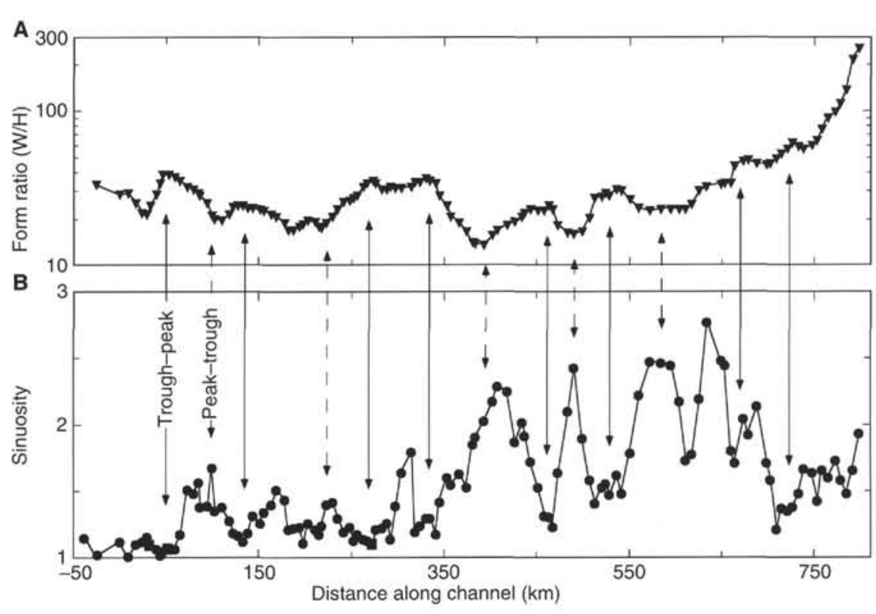

Figure 9. Correlation between channel form ratio (width:relief) and sinuosity. As in rivers, segments with higher sinuosity display a more pronounced V-shaped section. These variations are interpreted to reflect primarily the deepening of the channel talweg by entrenchment over the steeper valley slopes. The negative correlation demonstrates that entrenchment and aggradation of the talweg play an important role in maintaining grade. The increase of form ratio beyond 650 km is interpreted to reflect an overall increase in the size of the sediment forming the channel walls and levees.

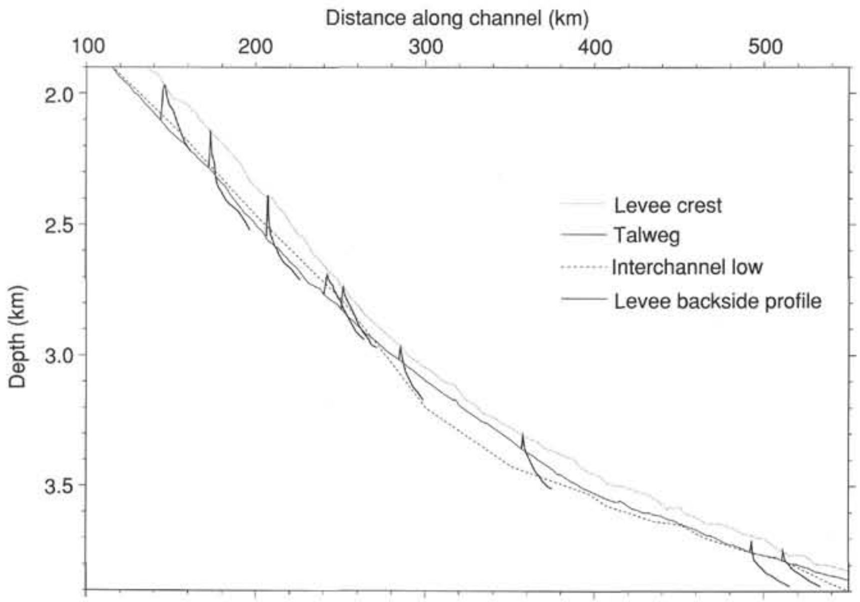

Figure 10. Levee backside topographic profiles (thick solid lines) compared with the longitudinal talweg depth profile (thin solid line), levee crest profile (thin dotted line) and interchannel depression (thin dashed line). The levee backside profiles follow the path of steepest descent and indicate the potential path of a parcel of flow stripped from the main channel. The backside profiles are projected on the same distance axis as the channel, although distance along the backside path was actually measured. Thus the backside profiles are not necessarily tangent to the interchannel low profile, which represents the average depth of the adjacent fan on each side of the channel. Note the small difference in topographic level between the backside and talweg on the upper fan profiles (up-fan of 300 km) and the marked contrast on the middle fan where the channel is highly sinuous and the talweg is perched.

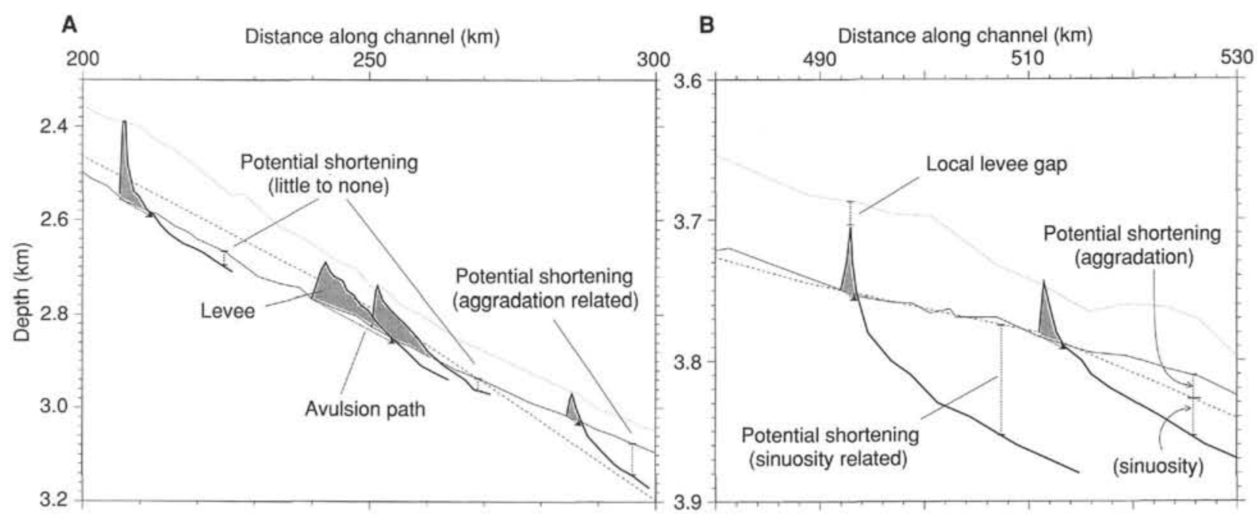

Figure 11. Detail of selected backside profiles illustrating the elements of a potential avulsion and associated effects. In **(A)** the channel is of relatively low sinuosity (~1.3; see Fig. 7B) and little or no base-level drop (shortening) would result from a bifurcation, except where the talweg becomes perched due to aggradation. For complete abandonment of the channel (avulsion) to occur, the backside path has to offer a topographic advantage in respect to the talweg depth profile (arrow). This generally implies the removal of a significant amount of levee sediment on the upper fan, where levees tend to be wider (shaded areas). **(B)** On the middle fan the potential base-level drop or shortening due to a bifurcation is large because the talweg tends to be perched and/or highly sinuous. Line patterns are the same as in Figure 10.

tion of the coarser sediment load after bifurcation, and development of a depositional foreset. Channel sinuosity downstream of the bifurcation is also anomalously low given that valley slope across the bifurcation site remains practically unchanged at ~3 m/km (Fig. 14B, -C). This indicates that the caliber of the sediment transported by the flows and deposited within the channel may bear a significant influence on the planform characteristics of the channel (Pirmez, 1994; Clark et al., 1992).

Middle and Upper Fan Bifurcations

Examples of three other channel bifurcations are shown in the bathymetric maps of Figure 15A–C. Here we focus on the development of the Purple and younger channel systems, with a brief account of the channel development prior to the Purple System. The overall fan stratigraphy and development of older channel systems is treated by Damuth et al. (1983b), Manley and Flood (1988), and Pirmez (1994).

Development of the Purple Valley

Three older channels are observed in the vicinity of the Purple bifurcation site (Fig. 15A). The Orange-1 Channel System has a subtle topographic expression to the west of Amazon Channel downstream of the Purple bifurcation site, and the older Orange-2 Channel extends to the east of Amazon Channel (Figs. 15A, 16). The Blue Channel is younger than the Orange-1 System and is located to the east (Figs. 3B, 16). The Orange-1 Channel (Orange Channel of Manley

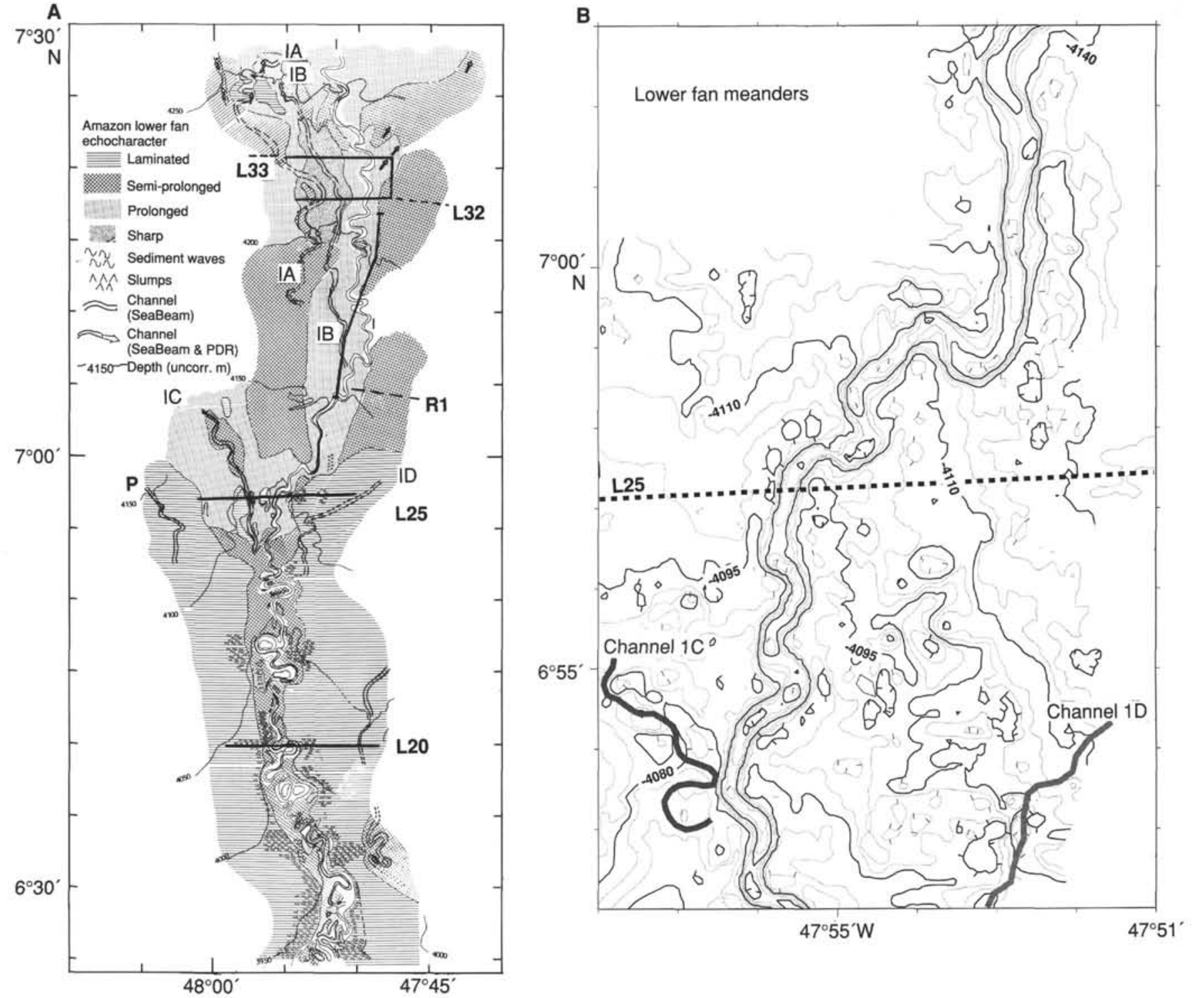

Figure 12. **A.** Bathymetry and acoustic echo character (based on 3.5-kHz profiles) of the lower portion of the fan. **B.** Detailed bathymetry near the 1C channel bifurcation. Note meander bend (cutoff loop?) of 1C Channel near bifurcation site.

and Flood, 1988) is located beneath the Purple-Amazon Channel near the Purple bifurcation site (Figs. 15A, 16). The Orange-1 Channel apparently bifurcated from the Orange-2 Channel farther upslope (Pirmez, 1994). The two channels are stratigraphically separated by a thick zone of acoustically chaotic reflections, interpreted as slump-debris-flow deposits (Unit R of Manley and Flood, 1988; Fig. 16). Unit R apparently originates within the Amazon Canyon area (Manley and Flood, 1988), but also involved failure and remobilization of overbank deposits of several channel systems, including the Orange-2 Channel (e.g., deep fault to the east in Fig. 16), and was locally eroded and overlain by the channel-overbank deposits of the Orange-1 System (Figs. 16, 17).

The Blue Channel System became established to the east of the Orange-2 System (Fig. 16). As the Blue System aggraded, overbank deposition extended to the west as far as the crest of the Orange-1 Channel. Local sediment failure and deformation is evident on the western flank of the Blue levee deposits (shallow faults in Fig. 16). The western levee of the Blue Channel is overlain by the distal deposits of the Purple Channel System, clearly establishing their relative stratigraphic position. However, the initial development of the Purple Channel may have been coeval with formation of the Blue System. The spatial separation of the two valleys, and the intervening topographic high of the Orange-1 Channel, precludes the establishment of a precise seismic stratigraphic relationship between the Blue and early Purple Channel Systems.

Purple Growth and Bifurcation

The Purple Channel bifurcated from the Blue Channel at about the 150-km mark (Fig. 3A). Amazon Channel departs from the Purple Channel near a sharp bend to the east at the 220-km mark (Purple bifurcation; Figs. 3B, 15A). The abandoned segment of the Purple Channel has a well-defined topographic expression up to about the −2520 m bathymetric contour where its western levee can be discerned from the levee of Amazon Channel (Fig. 15A). The talweg of the Purple Channel apparently had a sharp bend to the west near the

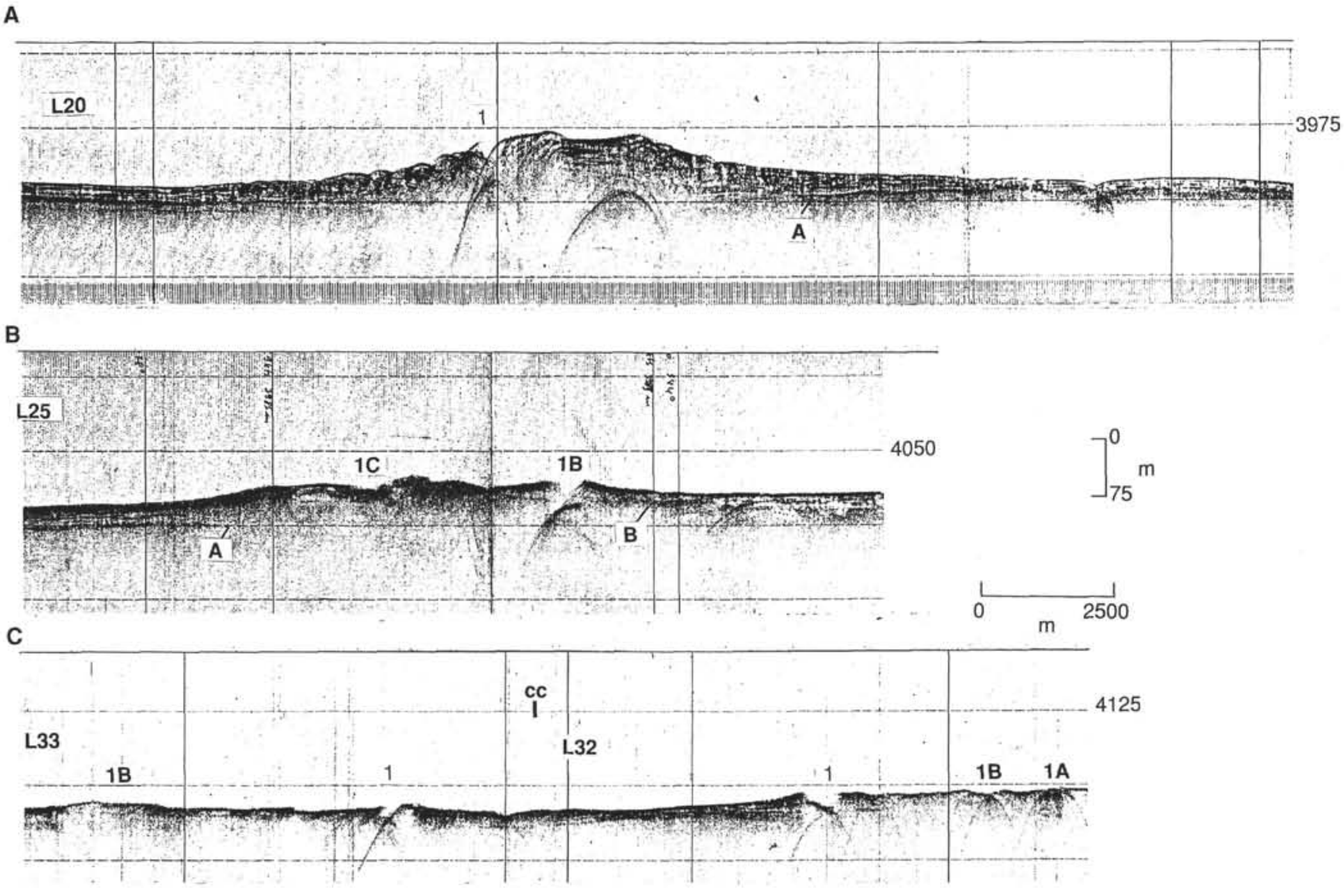

Figure 13. 3.5-kHz acoustic echograms crossing the lower portion of the channel (location in Fig. 12A). **A.** Upslope of 1C–1D bifurcation site (L20). **B.** Downslope of 1C bifurcation (L25). **C.** Lower Amazon Channel (L32). Note change in acoustic echo character on Amazon Channel levees from (A) to (B, C): levees are acoustically stratified upstream (line L20) and show progressively prolonged reflections downstream. Profile in (B) shows entrenchment of Amazon Channel into deposits associated with 1C and 1D channels. Reflection labeled "A" corresponds to the base of Amazon Channel upstream of the 1C bifurcation. Reflection labeled "B" marks the top of the 1C channel and appears to outcrop at the wall of Amazon Channel.

site of bifurcation, and this planform shape may have favored the bifurcation due to flows escaping the Purple Channel on the outer side of the meander bend.

The onset of Purple Channel development is characterized by prominent erosional truncation, in particular to the west of the Orange-1 Channel where the Purple System was initially established on the upper fan (Fig. 16). Erosional truncation and subsequent deposition of acoustically chaotic units are also observed on the eastern flank of the Orange-1 System. The Purple levee development is punctuated by the occurrence of intra-levee unconformities, characterized by sudden lateral changes in the position of downlap of overbank reflections, followed by renewed levee growth in a prograding and aggrading pattern (Fig. 16). On the western levee of the Purple System, these unconformities suggest an overall eastward migration of the levee crest. Sudden changes in levee geometry, associated with a shift of the position of downlap toward the channel, mark the growth of other levee systems as well (Blue Channel in Fig. 16, and younger channels discussed below).

The unconformity marking abandonment of the Purple System reveals erosional truncation on the eastern flank of the Purple levee by the Aqua Channel System as well as farther east (Fig. 16). The initial Aqua Channel became established immediately above the buried Orange-1 Channel, suggesting that this underlying system may have exerted some control on the position of the new channel. The morphology of the top-Purple unconformity suggests that the Purple Channel had a diminished relief prior to bifurcation (Fig. 16). Elsewhere along the abandoned segment of the Purple Channel there is evidence for acoustically transparent channel infill, but it is difficult to ascertain that the Purple Channel was filled prior to bifurcation (Pirmez, 1994). Downslope of the Purple bifurcation, the Aqua Channel System was established on the eastern flank of the Orange-1 Channel, which was overlain by the distal levee deposits of the Purple Channel (Fig. 17). The development of the Aqua overbank deposits was preceded by deposition of acoustically transparent and chaotic units interpreted as slump-debris-flow deposits related to the Purple bifurcation. These units were locally eroded by the initial Aqua Channel (Fig. 17, beneath the Amazon Channel levee).

Aqua Growth and Bifurcation

The Aqua Channel developed within a valley bounded by the Orange-1 Channel to the west and the Orange-2 Channel to the east (Figs. 15B, 17). The abandoned segment of the Aqua Channel departs from Amazon Channel near latitude 5°07′N (Fig. 15B). The Aqua Channel only displays a topographic expression farther downslope and is buried by the eastern levee of Amazon Channel in the vicinity of the bifurcation site. The Aqua channel growth is marked by several phases of overbank development, each with different geometric characteristics. The slump-debris-flow deposits associated with the Purple bifurcation (Fig. 17) apparently thin down-fan and are onlapped by high-amplitude reflections that form a lens-shaped deposit at the base of the Aqua System (Figs. 18, 19). This high-amplitude reflec-

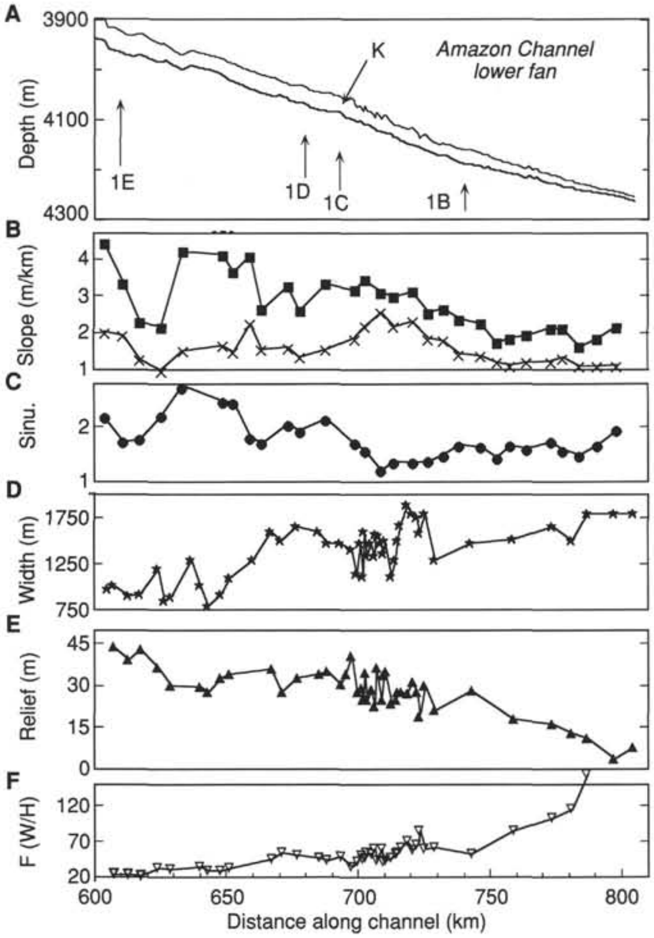

Figure 14. Amazon Channel morphologic parameters on the lower fan. K = knickpoint. In (B), ×'s = channel slope, squares = valley slope. Discussion in text.

tion packet (HARP; Flood et al., 1991) displays complex internal onlap and truncation suggesting it is composed of multiple small channels and lens-shaped deposits (Fig. 19, between base Aqua and DS horizons).

Initiation of overbank growth is separated from the HARP unit by a pronounced acoustic horizon onto which levee reflections terminate by downlap (Figs. 18, 19). This downlap surface is also characterized by a marked acoustic contrast, with overbank reflections displaying smaller acoustic amplitude in comparison to the HARP unit. Overbank reflections migrate progressively away from the channel axis in a progradational pattern. Above this progradational levee phase, the levees become more conformable and thin only gradually away from the channel, characterizing an aggradational levee-construction phase (Figs. 18, 19). The top of this conformable levee package is marked by extensive erosional truncation of the levee flanks and onlap. Onlapping units are characterized by acoustically chaotic reflections (e.g., to the north and east of the Aqua Channel; Figs. 18 and 19, respectively), and by nearly horizontal reflections to the west (Fig. 19) where the Brown System eventually developed. The western flank of the Aqua Channel was to be subsequently occupied by the Brown Channel System. Final abandonment of the Aqua Channel is marked, on the segment downstream of the bifurcation site, by a period of initial levee progradation followed by gradual infill (Fig. 19). The same progradational phase is detected upstream of the bifurcation site (Fig. 18).

We interpret these relations to indicate that channel bifurcation occurred during a pulse of increased turbidity-current influx, which led to increased overbank progradation accompanied by marked erosion of the levee backsides by overflowing turbidity currents (e.g., Fig. 16, to the east of Amazon Channel axis). Continued turbidity current activity led to levee growth and progradation of the Aqua levee with activity on the Brown valley to the west, as well as over the Aqua Channel System downstream of the bifurcation site. Once the Aqua Channel became completely filled, turbidity current activity switched entirely to the Brown valley (Fig. 19).

Brown Growth and Bifurcation

The Brown Channel developed in the depression bounded by the Aqua Channel to the east and the Orange-1 Channel to the west (Figs. 15B, 19). Farther downslope the thickness of the Orange-1 channel-levee system tapers down and the valley becomes topographically bounded to the west by the Purple Channel System (Figs. 20, 15B). The Brown Channel bifurcated at the 450-km mark, giving rise to the 1F and younger distributaries of Amazon Channel (Fig. 15C).

The Brown Channel System has a growth history similar to that of the other channels. Small channels with no apparent levees characterize the initial deposition and formation of a HARP unit. This HARP unit is best developed where fan gradient decreased and the valley widened (downslope of 5°25′N; Figs. 15B, 20). The upstream extension of the valley toward the bifurcation site is dominated by erosion of the underlying overbank deposits (Fig. 19; Pirmez, 1994). A pronounced downlap surface at the top of the HARP unit marks the onset of levee growth within the Brown valley (Fig. 20).

An unconformity within the levee separates the Brown from the 1F-Amazon phases of levee development (Fig. 20). Upstream of the bifurcation site the unconformity is characterized by a sudden change in levee geometry, with younger overbank reflections lapping against the older levee crests (Fig. 20). Downstream of the bifurcation site the end of deposition on the Brown Channel is characterized by a decrease in channel relief followed by widespread overbank deposition (Fig. 21). Channel abandonment was apparently preceded by partial channel filling, followed by increased sediment influx that led to overbank progradation and channel abandonment. Erosion of the Brown levee backside is clearly detected across the Brown bifurcation site (Fig. 21), but it is difficult to establish if downcutting occurred upslope after bifurcation.

The change in levee cross-sectional geometry detected at the intra-levee unconformity may reflect changes in channel planform geometry. The Brown Channel System was highly sinuous prior to the bifurcation (P ~ 3), and several, possibly cutoff, meanders occur within the abandoned segment of the channel (Fig. 15C). Meander cutoff must have occurred before or at about the same time as channel bifurcation occurred. The relatively small sinuosity of Amazon Channel across the bifurcation site (P ~ 1.5; Figs. 7B, 15C) suggests that planform sinuosity upstream of the bifurcation site decreased after bifurcation. A seismic line adjacent to the bifurcation site (Fig. 22) indicates that the nearly cutoff meander loop of Amazon Channel near the site of bifurcation formed after the abandonment of the Brown Channel. This suggests that changes in sinuosity upstream of the bifurcation site occurred in response to bifurcation. The presence of angular unconformities separating levee units with different external geometry further indicates that lateral channel migration and associated planform changes occurred rapidly.

Bifurcation Structure and Development of Longitudinal Profile

The Purple bifurcation led to the introduction of a steep segment on the profile, represented by the backsides of the Purple and Orange-1 Channel (Fig. 23). Slope below the knickpoint was of the order of

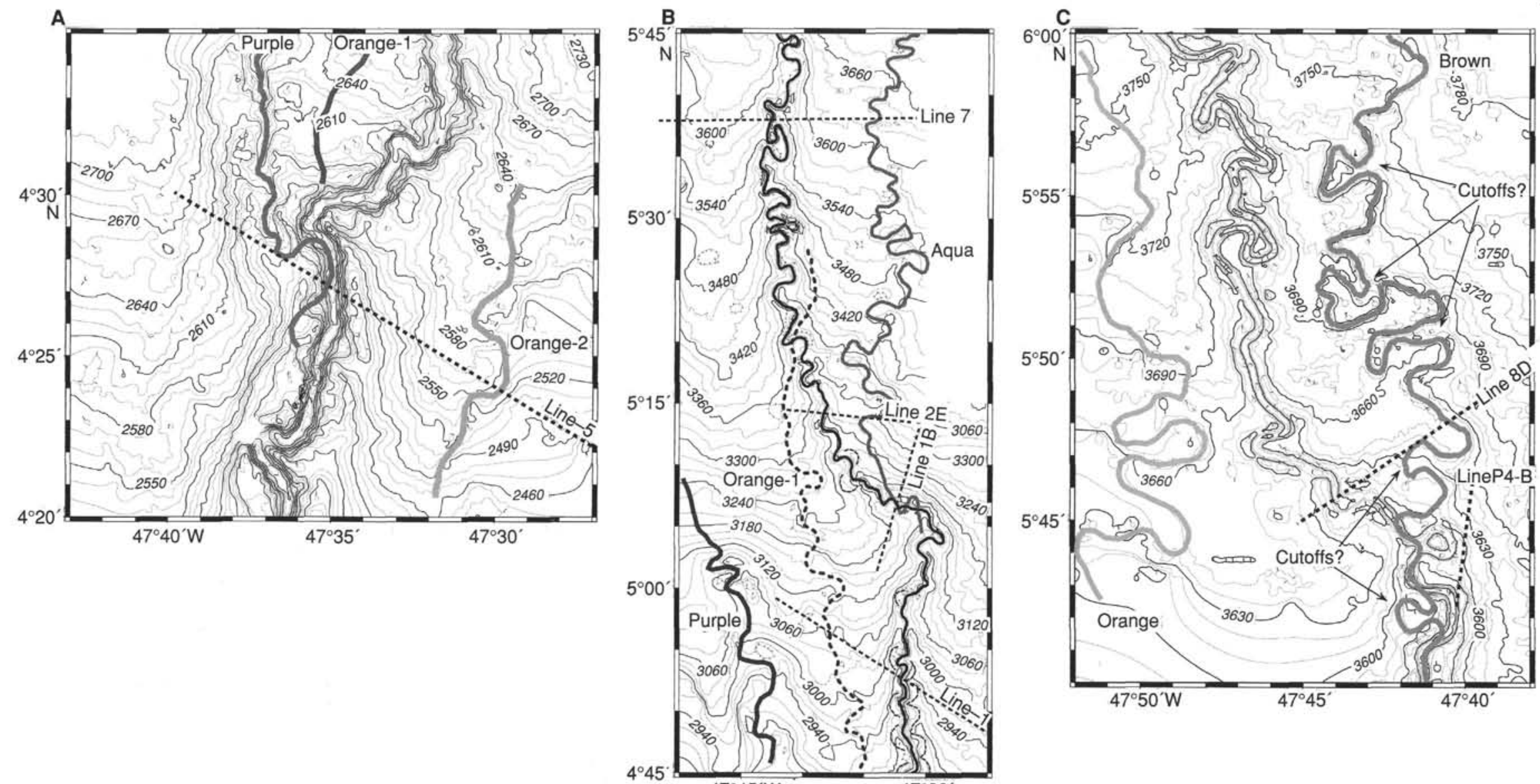

Figure 15. Bathymetry of channel bifurcations along Amazon Channel. The paths of older, partly buried channel systems were mapped from bathymetric and seismic reflection data (Pirmez, 1994). Seismic profiles are labeled with line numbers. Regions where data density precludes reasonable extrapolation of automatic contours are blanked. Data gridded and contoured using programs of Wessel and Smith (1991). **A.** Purple channel bifurcation. Note the apparent coincidence of the bifurcation site with the older Orange-1 Channel. **B.** Middle fan channel surrounding the Aqua bifurcation. Dashed lines adjacent to Amazon Channel mark levee crests associated with recent modification of the channel path. **C.** Brown Channel bifurcation. Note the highly sinuous nature of the abandoned Brown Channel (sinuosity of ~3) with several potential cutoff loops. A cutoff loop is inferred immediately upstream of the bifurcation site, suggesting lateral channel migration after avulsion (see text). All depths are in uncorrected meters. Contour interval and grid interval are, respectively, 10 m and 93 m (0.05 nmi) except for map in (B), where grid interval is 280 m (0.15 nmi) and contours are drawn every 20 m.

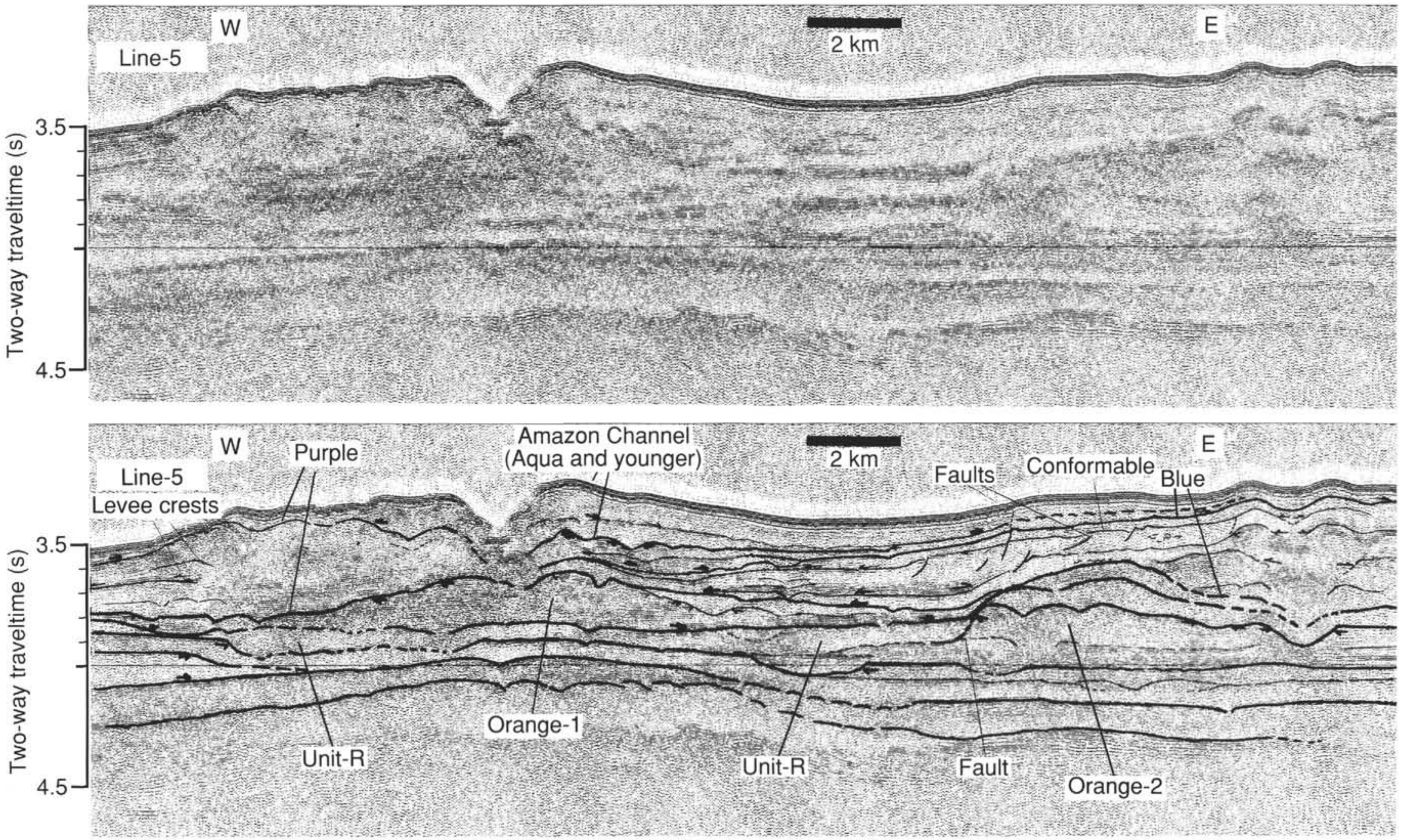

Figure 16. Interpreted seismic reflection profile immediately downstream of the Purple bifurcation site (location on Fig. 15A) with both interpreted (below) and non-interpreted (above) sections. Erosion of the Purple levee is inferred across the bifurcation site and to the east. Upper-half arrows mark reflection termination by onlap and downlap; lower-half arrows mark erosional truncation.

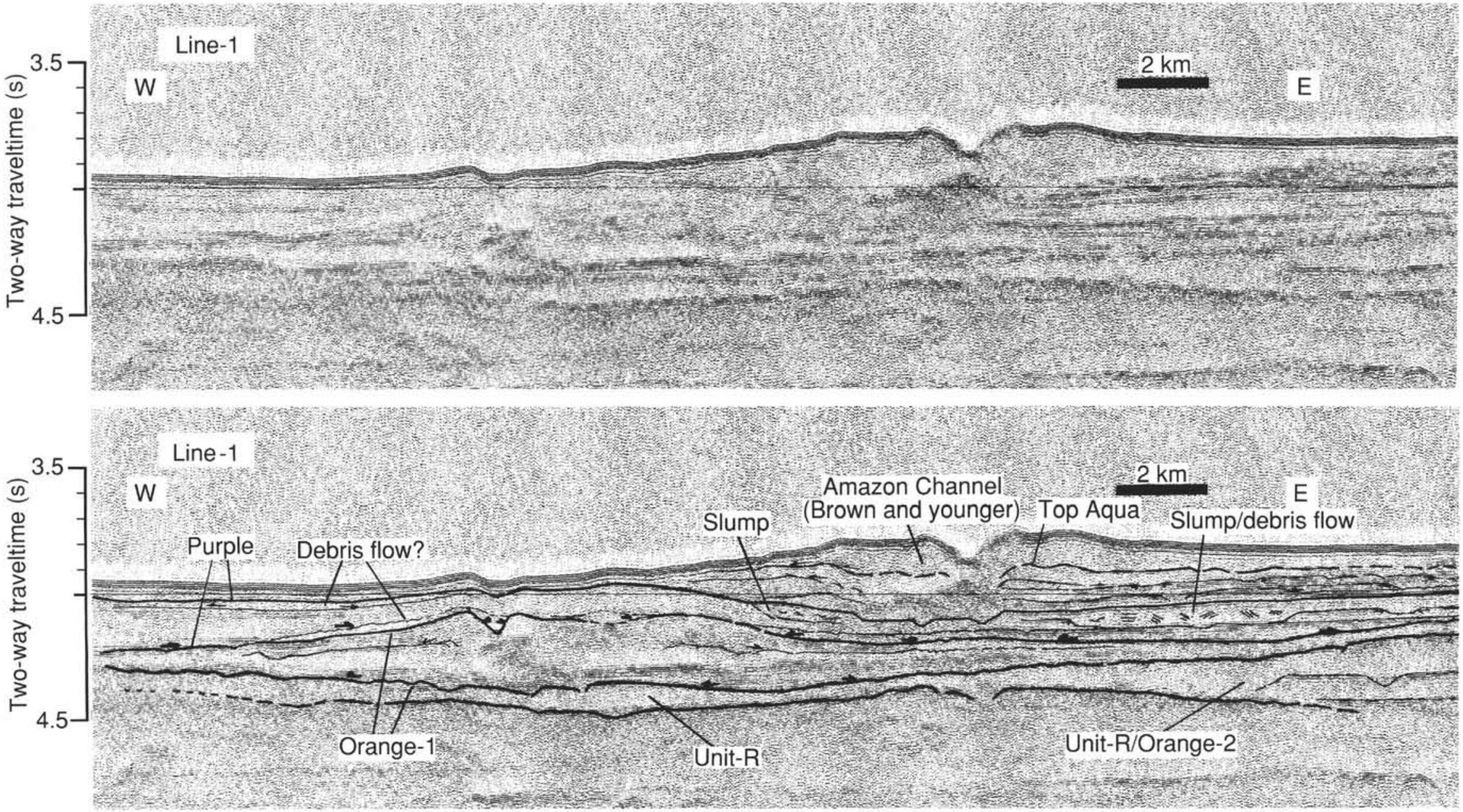

Figure 17. Interpreted seismic reflection profile downstream of Purple bifurcation (location in Fig. 15B) showing development of the Aqua and younger phases of Amazon Channel.

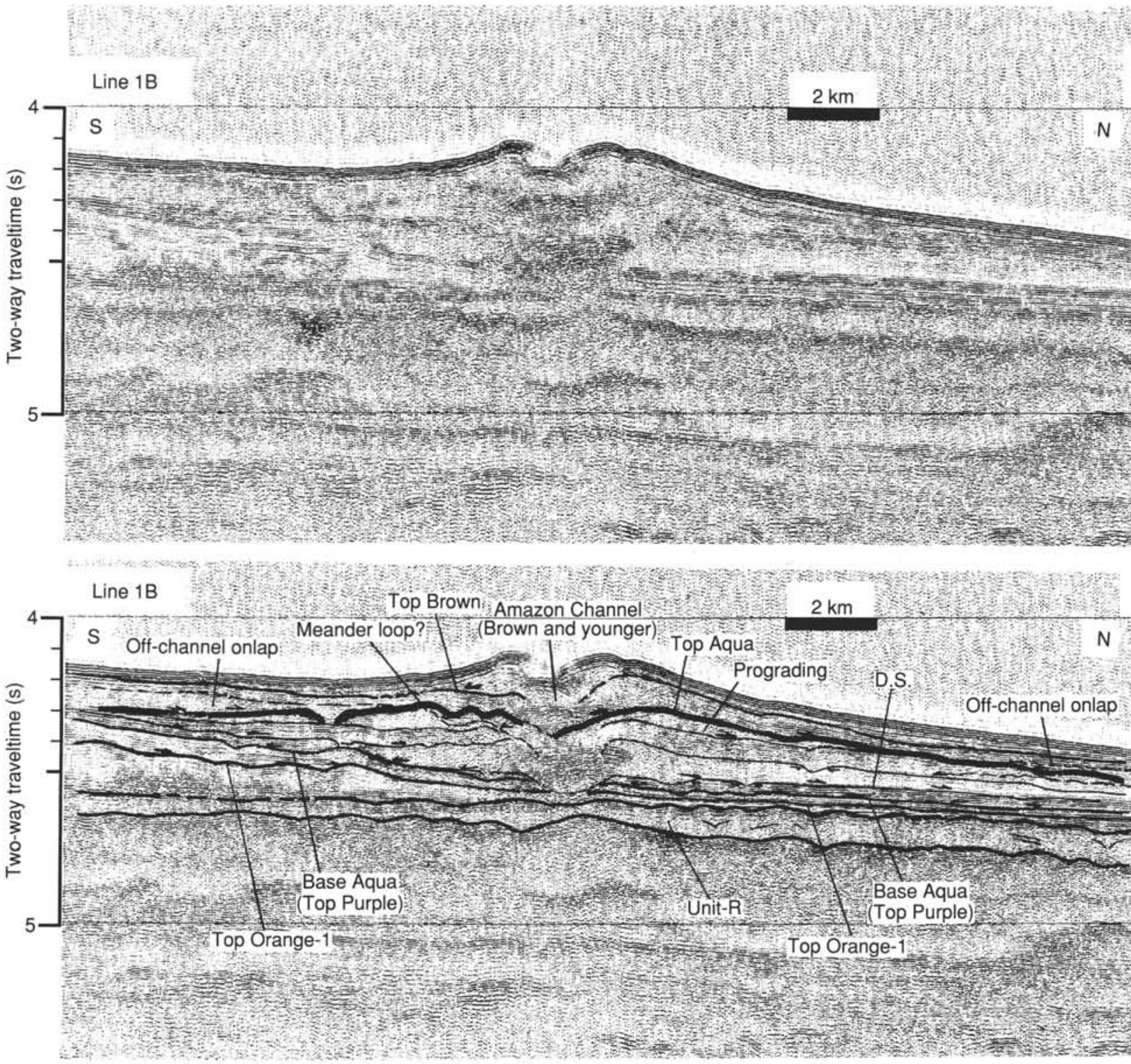

Figure 18. Interpreted seismic reflection profile immediately upstream of the Aqua bifurcation site (location in Fig. 15B).

30 m/km, whereas the abandoned Purple Channel had an average valley slope of about 8.5 m/km ($S_c \sim 6.5$ m/km, $P \sim 1.3$; Fig. 23). Amazon Channel valley gradient across the Purple bifurcation site is only 8–9 m/km but increases up to 11–12 m/km about 40 km upslope of the bifurcation site. The valley slope across the bifurcation site decreased significantly since the time of bifurcation, and the initial knickpoint apparently migrated upslope, given the steep valley observed upstream of the bifurcation site. It is not possible to determine the extent of headward downcutting from the seismic data, although it is apparent that significant erosion occurred on the backside of the Purple System immediately downstream of the bifurcation site (Fig. 16). In addition, the talweg of the abandoned segment of the Purple Channel (discounting the channel fill) is at a higher topographic level than the Amazon Channel talweg (Fig. 23), which indicates downcutting subsequent to Purple bifurcation. Adjustment to the knickpoint was further achieved by significant aggradation downstream of the bifurcation point within the Aqua valley (see below).

For the Aqua and Brown bifurcations there is also clear evidence of erosion on the backside of the abandoned channel, but we cannot demonstrate that talweg downcutting occurred upstream of the bifurcation site. The inferred depth of the Aqua Channel talweg upstream of the bifurcation site (from seismic data interpretation, e.g., Fig. 18 and Pirmez, 1994) suggests the presence of a knickpoint at 290 km (Fig. 24). This subsurface knickpoint is at about the same position where Amazon Channel valley slope increases to about 9 m/km (Fig. 7A). Nevertheless the slope on the levee backside of the Aqua Channel near the avulsion site reaches 15–18 m/km. This indicates that the valley slope of Amazon Channel, with pronounced peaks occurring upslope of the bifurcation sites, reflects the headward migration of the original knickpoint introduced at the time of bifurcation (Fig. 7A). The slope increase caused by each bifurcation can be assessed by comparing the pre-bifurcation channel slope with the slope across the knickpoint (Figs. 23–25). Based on the segment of the abandoned channel just downstream from the bifurcation site, the pre-bifurcation channel slope is estimated as 1.5 m/km, 4 m/km, and 6.5 m/km for the Brown, Aqua, and Purple channels, respectively. The pre-bifurcation sinuosity can be estimated from the surface trace of the abandoned channel segment (Fig. 15), and was about 3 for the Brown, 2.3

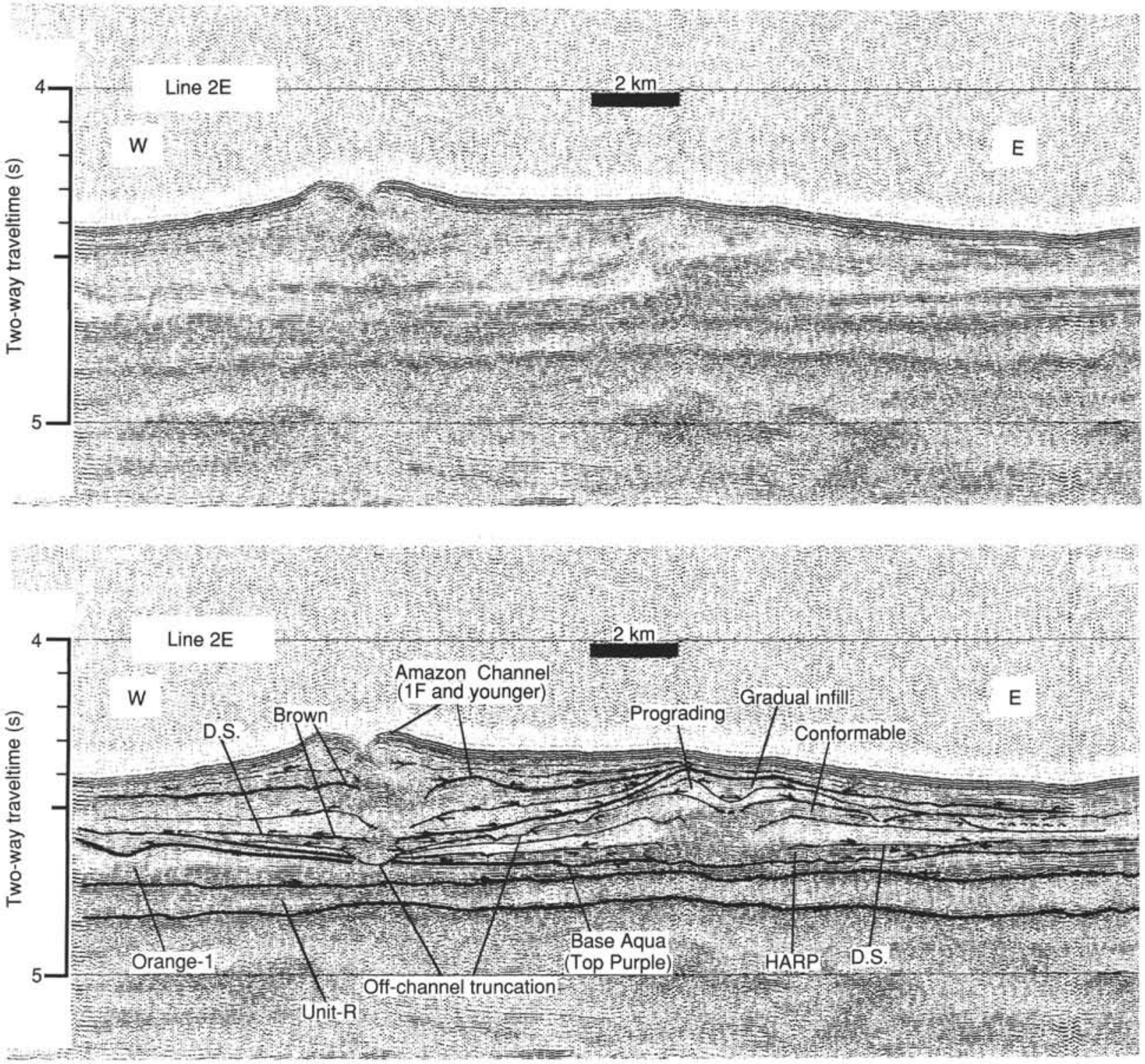

Figure 19. Interpreted seismic reflection profile downstream of Aqua bifurcation showing development of Brown and younger phases of Amazon Channel (location in Fig. 15B).

for the Aqua, and 1.3 for the Purple Channel. The average slope over the steep knickpoint at the time of bifurcation is estimated from the seismic data to be 8.5–12 m/km, 15–18 m/km, and 24–36 m/km, respectively, for the Brown, Aqua, and Purple channels.

The meandering nature of the Aqua and Brown channel systems indicates that the longitudinal profile may have been adjusted, at least in part, by changes in planform sinuosity upstream of the bifurcation site. Adjustment to a knickpoint in rivers occurs by headward erosion and downstream aggradation (Schumm, 1993). Headward erosion results in the propagation of a disturbance (knickpoint) upstream. As the knickpoint migrates headward, the depth profile upslope of the initial knickpoint position will become steeper, thus spreading the initial disturbance longitudinally away from the site of bifurcation. This increased slope can be achieved by downcutting of the talweg, by a decrease in channel sinuosity or by both. For instance, if the pre-bifurcation sinuosity is 2, and the slope below the knickpoint is twice the channel slope, headward migration of the knickpoint may be entirely adjusted by straightening of the channel. A much larger slope disturbance will require, in addition, that talweg elevation is reduced by entrenchment. Above we presented evidence for channel sinuosity changes upslope of the Brown bifurcation. Upstream of the Aqua Channel bifurcation, a series of arcuate levee crests adjacent to the channel appears to represent a more sinuous planform shape at an earlier phase of Amazon Channel (Fig. 15C). The exact timing of sinuosity changes is uncertain, but it occurred after bifurcation from the Aqua Channel (Pirmez, 1994).

A comparison between the thickness of channel and overbank deposits along Amazon Channel may provide additional insight into the mechanisms of profile adjustment. A summary of the measured thickness immediately upstream and downstream of the Purple, Aqua, and Brown bifurcations is presented in Figure 26. In all cases the total thickness downstream of the bifurcation site is either about the same or smaller than the talweg aggradation upstream of the site. However, the thickness upstream includes aggradation during one additional phase of channel development. For instance, the total talweg aggradation upstream of the Brown bifurcation site is 100 m,

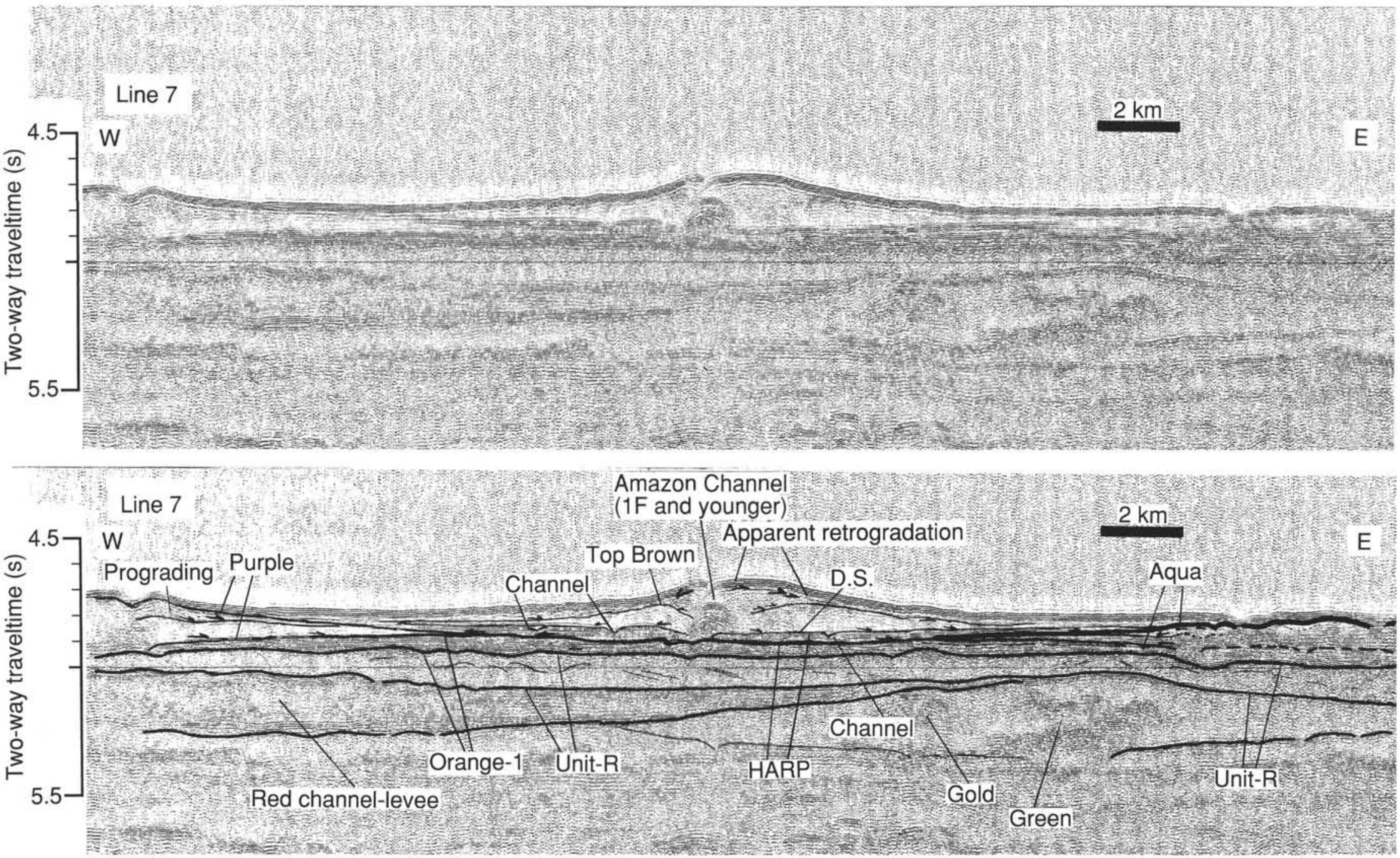

Figure 20. Interpreted seismic reflection profile showing development of the Brown and younger phases of Amazon Channel (location in Fig. 15B).

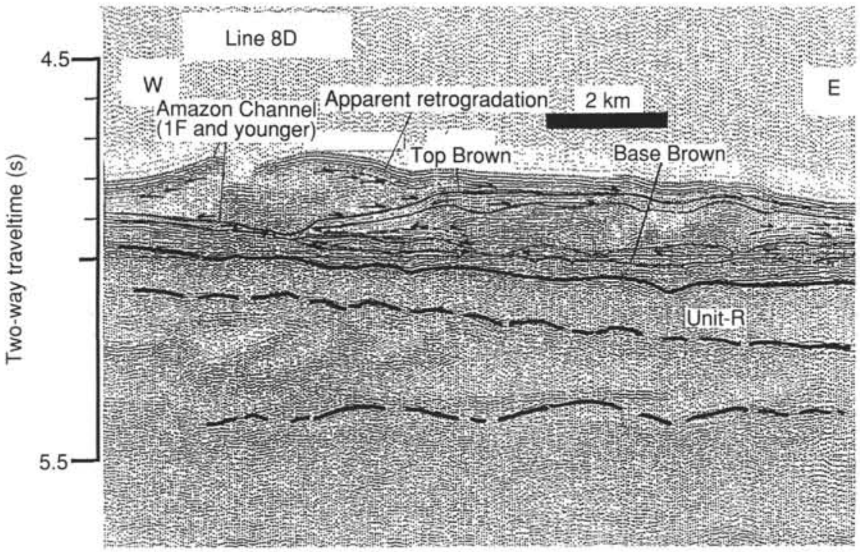

Figure 21. Interpreted seismic reflection profile immediately downstream of the Brown bifurcation site (location in Fig. 15C).

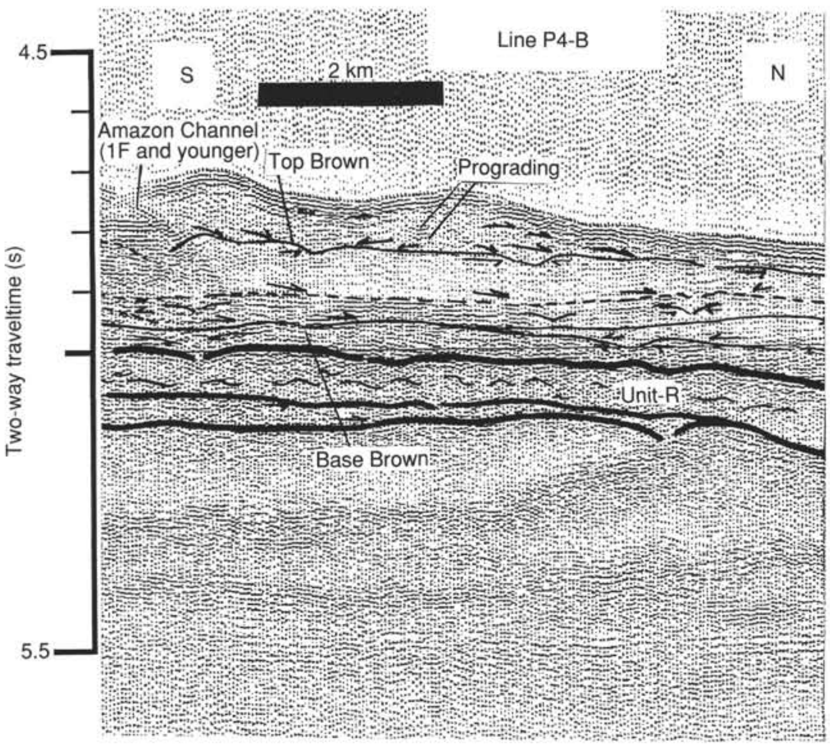

Figure 22. Interpreted seismic reflection profile (dip orientation, location in Fig. 15C) adjacent to Amazon Channel upstream of the Brown bifurcation site. Note that top Brown unconformity is overlain by overbank deposits associated with meander development with the Amazon Channel (post-Brown).

compared with 90 m downstream (Fig. 26A). The abandoned channel segment has a thickness of 65 m beneath the talweg; thus, assuming continuity across the bifurcation site, at least 65 m of the aggradation upstream was due to pre-bifurcation growth. After abandonment of the Brown System, the channel had a net aggradation of 35 m upstream of the bifurcation site and 90 m downstream (Fig. 26A). A similar situation is observed for the Aqua and Purple bifurcations (Fig. 26B, -C).

The abrupt increase in the thickness of post-bifurcation deposits requires that there was talweg downcutting upstream or at least, if no headward erosion occurred, that large quantities of sediment bypassed the talweg upstream of the bifurcation site. The levee crest shows a similar discontinuity in thickness (i.e., there was no significant levee aggradation upstream after bifurcation; Fig. 26A–C). This suggests that the flows traversing the region upstream and across the bifurcation sites produced relatively minor amounts of overbank deposition after bifurcation. This may be explained by either a deepening of the channel (entrenchment) or by an overall decrease in flow thickness during and after channel bifurcation.

DISCUSSION AND CONCLUSIONS

Amazon Channel growth is characterized by a continuous readjustment of several morphologic variables in response to varying flow conditions. When traversing a steeper fan valley, the channel becomes more sinuous and cuts down into the talweg. Conversely, when the valley slope decreases, the channel tends to be less sinuous and shallower, apparently indicating aggradation of the talweg at the expense of the levees. Both changes in talweg elevation and planform

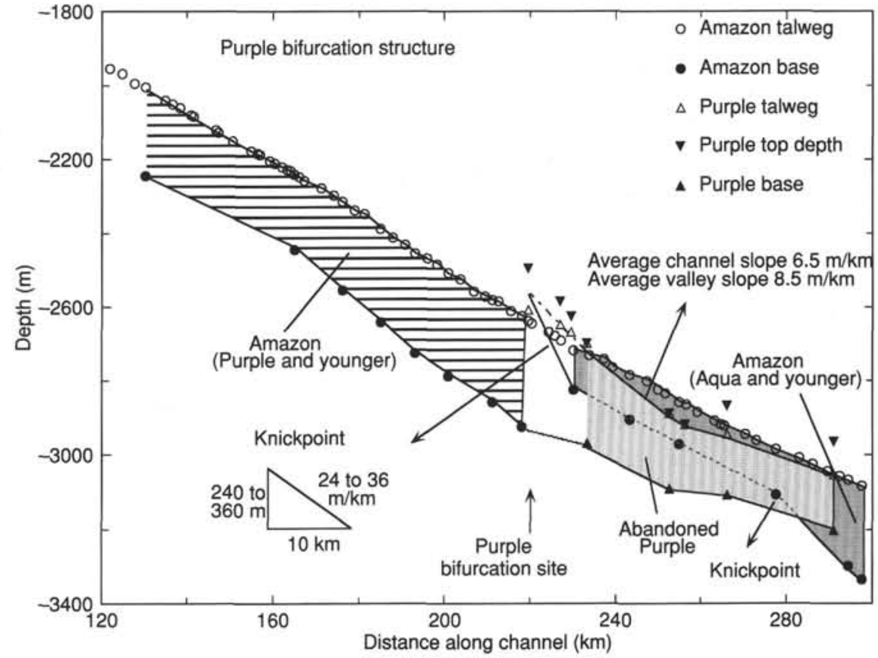

Figure 23. Longitudinal structure profile of the Purple bifurcation, showing depth of talweg on Amazon Channel, and top (talweg) and depth of basal unconformity on abandoned Purple channel. Thick line represents the bifurcation path and was used to estimate average slope of knickpoint introduced by bifurcation. Discussion in text.

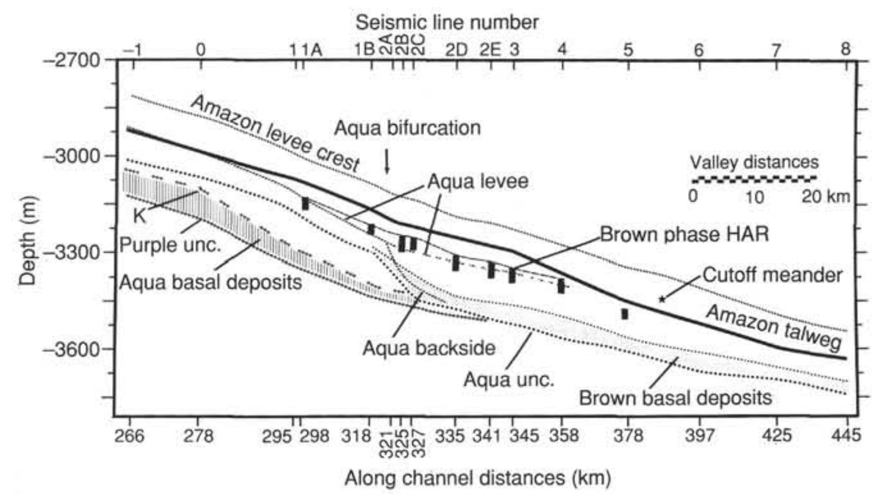

Figure 24. Longitudinal structure profile of the Aqua bifurcation, showing depth to talweg on Amazon Channel, and top (talweg and levee crest) and depth to basal unconformity on abandoned Aqua Channel. Intermediate surfaces shown are the top of basal deposits (HARP) within the Aqua and Brown systems and the projected topography of the Aqua levee backside. Profile is drawn with respect to distance on a straight line following the overall trend of Amazon Channel; corresponding along-channel distances form an irregular scale because of the channel sinuosity. Seismic line crossings are indicated on the top axis (numbers shown in figures above). Discussion in text.

sinuosity play a role in maintaining a smooth longitudinal depth profile, but the relative importance of each of these processes appears to depend on several variables, particularly valley slope and the nature of the sediment load carried by the flow and deposited within the channel perimeter (Damuth et al., 1988; Clark et al., 1992; Pirmez, 1994).

Meander development in rivers depends on a delicate balance between the available flow power and the resistance of the substrate to erosion (Richards, 1982), and similar principles probably also apply to submarine meanders (Pirmez, 1994). At steeper valley slopes, presumably higher flow velocities exceed the erosion threshold of the channel sediments, and slope adjustment is achieved primarily via entrenchment (e.g., near knickpoints, or on the upper fan where valley slope is large). At smaller slopes the flows tend to deposit their loads, and an increase in sinuosity would lead to a further decrease in their competence. The lower fan channel talweg still cuts below the adjacent fan surface, but small-scale aggradation (channel filling?) leads to frequent channel switching (Figs. 1, 12A).

The role of the type of sediment on planform morphology is particularly evident on the lower fan surface where the coarser sediment appears to be partly responsible for the smaller sinuosity (Fig. 12A). Presumably, the morphologic parameters of Amazon Channel reveal a balance between particular flow conditions and the available sediment. An increase of flow discharge (flow velocity, density) or of dominant grain size may force a change of equilibrium conditions. Such a change may, for instance, shift the gradients where high sinuosity channels develop higher values (Pirmez, 1994).

Channel-levee aggradation and meandering leads to an intrinsically unstable equilibrium, because eventually there is a shorter and more efficient route to dissipate flow energy via the levee backsides. This concept is similar to the idea of base level in fluvial geomorphology. A river channel on a flood plain eventually avulses, with the new channel seeking a shorter route to the sea (Schumm, 1977; 1993). The amount of base-level drop, or equivalently the amount of stream shortening, will depend on the relative elevation of the parent channel in respect to the flood plain and on the pre-avulsion sinuosity (Fig. 11A, -B). Base level for a channelized turbidity current is ultimately the deepest point within the basin. This point does not change depth significantly during the relatively short-lived history of an individual fan channel, but through channel bifurcation a shorter route is sought

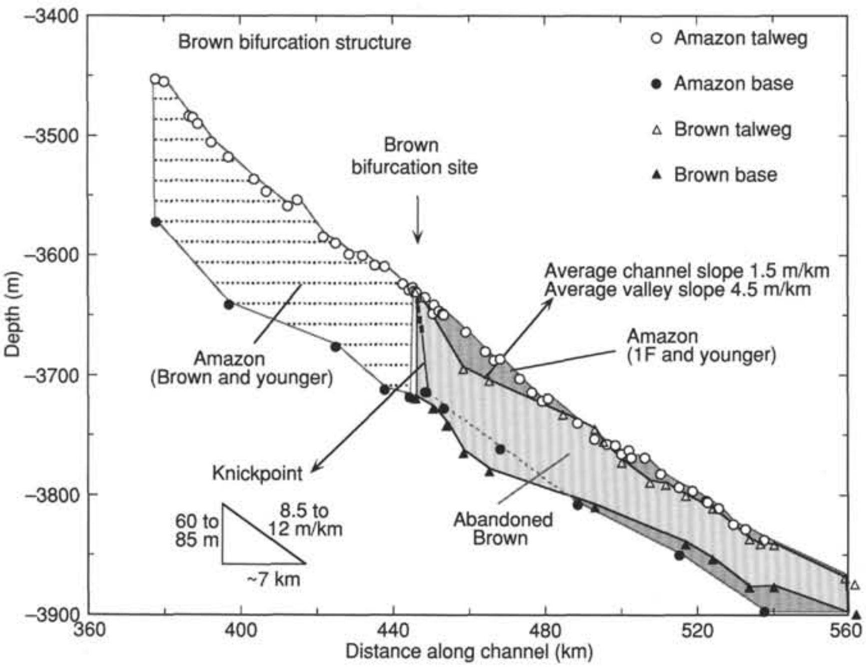

Figure 25. Longitudinal structure profile of the Brown bifurcation, showing depth to talweg on Amazon Channel, and top (talweg) and depth to basal unconformity on abandoned Brown channel. Thick line was used to estimate average slope of knickpoint introduced by bifurcation. Discussion in text.

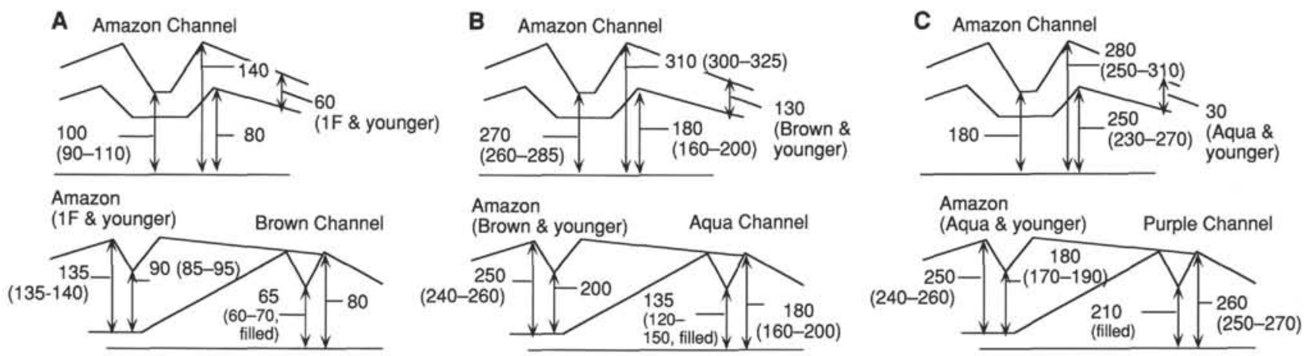

Figure 26. Comparison of thickness beneath levee crest and talweg across bifurcation sites. **A.** Brown bifurcation. **B.** Aqua bifurcation. **C.** Purple bifurcation. Discussion in text.

by the flows that may eventually reach that point. The amount of shortening is quantified through the ratio between the slope of the parent channel and that of the new channel after avulsion. The Purple, Aqua, and Brown bifurcations represented an average shortening of the channel of the order of 3.5 to 5, 4 to 4.5, and 6 to 8, respectively. The maximum shortening associated with the Brown System reflects a combination of high pre-bifurcation sinuosity and topographic aggradation. The shortening is in all cases larger than the pre-bifurcation sinuosity of 1.4, 2.3, and 3, respectively, for the Purple, Aqua, and Brown systems.

The response of the channel morphology to bifurcation will depend on the amount of shortening imposed, but other factors, such as the absolute slope and pre-bifurcation sinuosity, also play a role. For instance, significant entrenchment occurred across the Purple bifurcation, where the initial channel had a small sinuosity and little shortening could be accomplished by channel straightening. The knickpoint at the Purple bifurcation is the most significant of the bifurcations examined along Amazon Channel (Fig. 23), and the channel was highly aggraded due to stacking of the Purple and Orange-1 channels, and possibly to pre-bifurcation channel fill. On the other hand, significant slope adjustment occurred by a sinuosity decrease upslope of the highly meandering Brown Channel, even though maximum shortening occurred there.

The Rhône Fan channel provides a "snapshot" for the morphology of a middle-upper fan channel bifurcation (Droz and Bellaiche, 1985; O'Connell et al., 1991), and the apparent channel response to bifurcation may be compared to observations on Amazon Channel. The marked channel entrenchment was apparently the result of a very large shortening imposed by the bifurcation. On the upper-middle fan several phases of channel development are vertically stacked leading to high topographic aggradation (Droz and Bellaiche, 1985). In addition, pre-avulsion infilling of the channel (O'Connell et al., 1991) led to additional elevation difference between the talweg and the adjacent valley. The abandoned portion of the channel is moderately sinuous ($P \sim 2.3$) and had a channel slope of about 2 m/km (according to maps in Droz and Bellaiche, 1985). In contrast, the levee backsides show a slope of the order of 50 m/km, and the interchannel depression was several hundred meters below the channel talweg. Thus the shortening imposed (~25) could not be accommodated by straightening of the channel alone. The upslope portion of the system shows a relatively low sinuosity, with the entrenched meanders apparently influenced by the indurated sediments within the channel fill (O'Connell et al., 1991).

The amount of headward entrenchment cannot be easily quantified on Amazon Channel, in particular because of the difficulty of interpreting seismic reflection data below the channel axis (Flood, 1987). Nevertheless there is direct evidence from the present-day channel cross-sectional shape (Fig. 9), and from interpretation of seismic data near the bifurcation sites (Figs. 16, 19, 21), that channel entrenchment is a common response of the system to steeper gradients along the fan. The final adjustment to an equilibrium profile is achieved by significant downstream aggradation, as revealed by the abrupt increases in the thickness of channel and levee deposits across the bifurcation sites. The thickness variations indicate that the channel system was dominated by sediment bypass during and after bifurcation. This is interpreted to indicate that channel bifurcations occurred during times of increased sediment discharge and marked progradation of the channel system.

The development of a channel following a bifurcation is marked by two distinct depositional units. The base of a channel system is an unconformity characterized by erosional truncation and onlap by acoustic units interpreted as slump-debris-flow deposits, and lobe-like deposits produced by the lateral spreading of turbidity currents issued from unleveed channels. This basal unit was termed a HARP on the basis of seismic facies by Flood et al. (1991). Erosional truncation is particularly prominent on the backside of the abandoned channel-levee in the vicinity of the bifurcation site, and possibly extends headward within the channel upslope of the bifurcation site. Erosion also occurs locally on the backsides of the channel upslope of the bifurcation site, indicating that bifurcation was marked by extensive overbank flow (e.g., Figs. 16, 18). Channel and overbank deposits prograde over this basal HARP unit, defining a downlap surface that is particularly prominent away from the channel axis. A sudden change in acoustic facies and depositional geometry marks the separation between HARP and overbank deposits. We think that the apparently abrupt onset of channel-levee development is related to an increase in the proportion of fine-grained sediment (primarily clays) carried by the flows, associated with a more stable channel position. A more stable channel position would be due to the presence of more cohesive sediments and increased channel relief, leading to a self-reinforcing cycle of channel aggradation and levee growth.

Several factors may be responsible for a change in the flow characteristics and in the nature of the sediment load inferred to occur at the onset of channel-levee growth. Sea-level control on the grain size distribution of the sediment delivered at the canyon mouth is one possibility (Posamentier et al., 1991). As the rate of sea-level fall increases, base-level fall in the fluvial system leads to stream rejuvenation and eventual increase in the sand:mud ratio of the sediment delivered at the river mouth. As the rate of fall decreased and the river eventually attains a graded profile, the rates of erosion decreased leading to a decrease in the sand:mud ratios. A rise of sea level would lead to landward migration of the source with consequent decrease in the total amount and grain size of sediment available for turbidity currents. A similar concept may be applied to the equilibrium profile of Amazon Channel. After bifurcation, headward migration of a knickpoint would lead to talweg entrenchment and to a decrease in planform sinuosity, consequently increasing the sediment input into the new valley. Reworking of older channel fill deposits will likely involve the coarsest sediments available in the system, leading to an increase in the sand:mud ratio of the sediment load delivered to the new valley. The rate of headward erosion and downcutting should decrease through time as the initial slope disturbance is smoothed. Whereas it is possible that such an internal control plays a significant role in the development of the observed sequences, the evidence from levee thickness changes and acoustic stratal patterns near channel bifurcations presented here suggests that channel bifurcation occurred as a result of an increase in flow and sediment discharge to the system. Thus, internal feedback mechanisms such as the adjustment of the submarine channel graded profile and the interaction between channel relief and overbank flow probably play an important role in the sediment distribution, but channel growth is ultimately controlled by external influences on the sediment flux into the channel. It is uncertain whether changes in sediment influx to the fan occur in response to a relative fall in sea level, or to variations in river discharge, climate, or even local phenomena at the river mouth such as delta-channel switching. It appears that, given the large influx of sediment from the Amazon River and apparently rapid growth of the fan (Flood et al., 1991; Pirmez, 1994), individual channel-levee systems may record changes in sediment influx to the fan occurring at periods of a few thousand years or less.

ACKNOWLEDGMENTS

Financial support for the acquisition, processing, and analysis of the data used in this study was provided by the National Science Foundation (NSF grants OCE 81-17469, OCE 82-14819, OCE 86-01002, OCE 88-17812), Joint Oceanographic Institutions, Inc. (JOI grant JSC-1592). Additional support was provided to C.P. by the Conselho Nacional de Desenvolvimento Científico e Tecnológico-CNPq of Brazil, Universidade Federal Fluminense-UFF, and the Department of Geological Sciences of Columbia University. We thank J.E. Damuth, N.W. Driscoll, D.E. Hayes, R.O. Kowsmann, P.L. Manley, J.P. McGinnis, W.B.F. Ryan, and D. Twichell for valuable discussions and suggestions to improve earlier versions of this manuscript. Reinhardt Hesse, Patricia L. Manley, David J.W. Piper, and Fabio Trincardi provided constructive comments that improved the manuscript. This is L-DEO contribution 5279 and MSRC contribution 980.

REFERENCES*

Clark, J.D., Kenyon, N.H., and Pickering, K.T., 1992. Quantitative analysis of the geometry of submarine channels: implications for the classification of submarine fans. *Geology,* 20:633–636.

Damuth, J.E., Flood, R.D., Kowsmann, R.O., Belderson, R.H., and Gorini, M.A., 1988. Anatomy and growth pattern of Amazon deep-sea fan as revealed by long-range side-scan sonar (GLORIA) and high-resolution seismic studies. *AAPG Bull.,* 72:885–911.

Damuth, J.E., Kolla, V., Flood, R.D., Kowsmann, R.O., Monteiro, M.C., Gorini, M.A., Palma, J.J.C., and Belderson, R.H., 1983a. Distributary channel meandering and bifurcation patterns on Amazon deep-sea fan as revealed by long-range side-scan sonar (GLORIA). *Geology,* 11:94–98.

Damuth, J.E., Kowsmann, R.O., Flood, R.D., Belderson, R.H., and Gorini, M.A., 1983b. Age relationships of distributary channels on Amazon deep-sea fan: implications for fan growth pattern. *Geology,* 11:470–473.

Droz, L., and Bellaiche, G., 1985. Rhône deep-sea fan: morphostructure and growth pattern. *AAPG Bull.,* 69:460–479.

Flood, R.D., 1987. Side echoes from a sinuous fan channel obscure the structure of submarine fan channel-levee systems, Amazon fan. *Geo-Mar. Lett.,* 7:15–22.

Flood, R.D., and Damuth, J.E., 1987. Quantitative characteristics of sinuous distributary channels on the Amazon deep-sea fan. *Geol. Soc. Am. Bull.,* 98:728–738.

Flood, R.D., Manley, P.L., Kowsmann, R.O., Appi, C.J., and Pirmez, C., 1991. Seismic facies and late Quaternary growth of Amazon submarine fan. *In* Weimer, P., and Link, M.H. (Eds.), *Seismic Facies and Sedimentary Processes of Modern and Ancient Submarine Fans:* New York (Springer-Verlag), 415–433.

Garrison, L.E., Kenyon, N.H., and Bouma, A.H., 1982. Channel systems and lobe construction on the Mississippi Fan. *Geo-Mar. Lett.,* 2:31–39.

Manley, P.L., and Flood, R.D., 1988. Cyclic sediment deposition within Amazon Deep-Sea Fan. *AAPG Bull.,* 72:912–925.

Moyes J., Gayet, J., Poutiers, J., Pujol, C., and Pujos-Lamy, A., 1978. Étude stratigraphique et sédimentologique. *In* Combaz, A., and Pelet, R. (Eds.),

*Abbreviations for names of organizations and publications in ODP reference lists follow the style given in *Chemical Abstracts Service Source Index* (published by American Chemical Society).

Géochimie des Sédiments Marins Profonds, Orgon II, Atlantique N-E, Brésil: Paris (Éditions du CNRS), 105–156.

Nittrouer, C.A., Kuehl, S.A., DeMaster, D.J., and Kowsmann, R.O., 1986. The deltaic nature of Amazon shelf sedimentation. *Geol. Soc. Am. Bull.,* 97:444–458.

O'Connell, S., Normark, W.R., Ryan, W.B.F., and Kenyon, N.H., 1991. An entrenched talweg channel on the Rhone Fan: interpretation from a Sea-Beam and Seamarc I survey. *In* Osborne, R.H. (Ed.), *From Shoreline to Abyss: Contributions in Marine Geology in Honor of Francis Parker Shepard.* Spec. Publ.—Soc. Econ. Paleontol. Mineral., 46:259–270.

Pirmez, C., 1994. Growth of a submarine meandering channel-levee system on the Amazon Fan [Ph.D. thesis]. Columbia Univ., New York.

Posamentier, H.W., Erskine, R.D., and Mitchum, R.M., Jr., 1991. Models for submarine fan deposition within a sequence-stratigraphic framework. *In* Weimer, P., and Link, M.H. (Eds.), *Seismic Facies and Sedimentary Processes of Modern and Ancient Submarine Fans:* New York (Springer-Verlag), 127–136.

Richards, K., 1982. *Rivers: Form and Processes in Alluvial Channels:* London (Methuen).

Schumm, S.A., 1977. *The Fluvial System:* New York (Wiley).

————, 1993. River response to baselevel change: implications for sequence stratigraphy. *J. Geol.,* 101:279–294.

Weimer, P., 1989. Sequence stratigraphy of the Mississippi Fan (Plio-Pleistocene), Gulf of Mexico. *Geo-Mar. Lett.,* 9:185–272.

————, 1991. Seismic facies, characteristics, and variations in channel evolution, Mississippi Fan (Plio-Pleistocene), Gulf of Mexico. *In* Weimer, P., and Link, M.H. (Eds.), *Seismic Facies and Sedimentary Processes of Modern and Ancient Submarine Fans:* New York (Springer-Verlag), 323–347.

Wessel, P., and Smith, W.H.F., 1991. Free software helps map and display data. *Eos,* 72:441–446.

Ms 155IR-103